4
Convection

http://www.staff.science.uu.nl/~delde102/AtmosphericDynamics.htm

"We try to use the word *heat* as little as possible, sometimes as an adjective, as in *heat transfer*, energy transfer resulting from temperature differences, but never as a noun. Not much more than a century ago heat was looked upon as a substance, a massless, colorless, odorless fluid called *caloric*. According to the caloric theory, bodies were heated because of the passage of caloric from one to another. … Although most textbooks officially acknowledge the death of caloric, they then proceed to do everything possible to breathe life into its corpse. Vestiges of the caloric theory remain in phrases such as "the amount of heat added to, or absorbed by, a body", in thermodynamic quantities such as heat capacities, and so on. We do not use the word *heat* in the sense of saying that heat is added to a system. Instead we say that the system is heated".

"**Atmospheric Thermodynamics**", by C.F. Bohren and B.A. Albrecht, Oxford University Press, 1998, 402 pp. (p. 24-25)

4.1 Static instability and shallow convection

Craig Bohren and Bruce Albrecht are right in saying that "heat" is not a noun (see quote above), but it should be added that, by using the term "heat capacity", even these authors cannot avoid to "breath life into the corpse", which indicates that vestiges of the caloric theory of heat are still very well entrenched in our professional language, as this chapter again demonstrates.

This chapter discusses the formation of "puffy" or "piled" clouds, which are named **cumulus clouds**. These clouds form as a result of **instability of hydrostatic balance** (static instability) (section 1.15), which is aided by "**release of latent heat**"[147] when water vapour condenses in updraughts or when water droplets freeze. The associated vertical circulations are collectively known as **"convection"**.

[147] note that we have sinned here also

FIGURE 4.1. Left panel: fair weather cumulus over Washington D.C. (Copyright : Natalia Weber). Right panel: cumulus clouds with precipitation in summer over New Mexico. Copyright : Will Miller. Source: http://cloudappreciationsociety.org/.

Conversely, when precipitation (rain) falls and evaporates below cloud base, latent heat is "consumed". This cools the air below cloud base, hence reducing the buoyancy of the rising air, which feeds the cloud, thus reducing the lifetime of the cloud. The cumulus clouds over Washington D.C., shown in the left panel of **figure 4.1**, are non-precipitating. The clouds over New Mexico, shown in the right panel of **figure 4.1** are producing precipitation.

Satellite images reveal that there is a surprising degree of organization in the distribution of cumulus clouds, especially over the ocean during outbreaks of polar air. In the case illustrated in **figure 4.2**, air is flowing from the ice-edge over a relatively warm sea-surface., while it is vigorously heated from below, thereby creating a statically unstable temperature stratification (potential temperature decreases with increasing height). When the resulting convection currents reach the lifting condensation level clouds appear. In the first instance these clouds are almost invariably organized into " **cloud streets**" (two-dimensional cells) oriented in the direction of the "background" wind. After the air has been flowing over sea for a while the cloud-streets break up and three-dimensional cellular patterns develop. In many cases these three-dimensional cloud patterns consist of an array of cells in which a thin ring of clouds surrounds a large cloud-free area. These cells are called **"open cells"** (see also **figure 4.3**).

Also possible are so-called **"closed cells"**, which are complementary to open cells. In closed cells the clouds are concentrated in the middle of the cell and are surrounded by a clear area. The degree of cloud cover in closed cells is generally much larger than in open cells, hence the terms "open" and "closed".

Theoretical and numerical model studies indicate that convective pattern selection is related to the vertical shear in the background wind [148], as well as the shape of the "static" (in the absence of convection) temperature profile $\theta_0(z)$ [149]. Cloud streets are preferred with strong vertcal shear, open cells are preferred when vertcal shear is weak and the greatest static instability is located adjacent to the lower boundary, whereas closed cells are preferred

---

[148] Asai, T., 1970a: Three-dimensional features of thermal convection in plane Couette flow. **J.Meteor.Soc.Japan**, 48, 18-29.

Asai, T., 1970b: Stability of plane parallel flow with variable vertical shear and unstable stratification. **J.Meteor.Soc.Japan**, 48, 129-139.

[149] Van Delden, A., 1988: On the flow-pattern of shallow atmospheric convection. **Beitr.Phys.Atmos.**, 61, 169-186.

when the greatest static instability is located adjacent to the upper boundary. The (shape of the) "static" temperature profile is determined by processes other than convection, such as diabatic heating (due to radiation and latent heat release), large scale vertical motion and changing (lower) boundary conditions. The transition from streets (or rolls) to open cells, seen in **figure 4.2**, is probably determined by the reduction of the shear in the background flow and by the steadily increasing sea-surface temperature as the air flows southwards. The latter effect induces a static temperature profile that is extremely unstable near the sea-surface. This favours the transition to open cells. Radiative cooling at cloud top is probably of great importance, especially in the case closed cells.

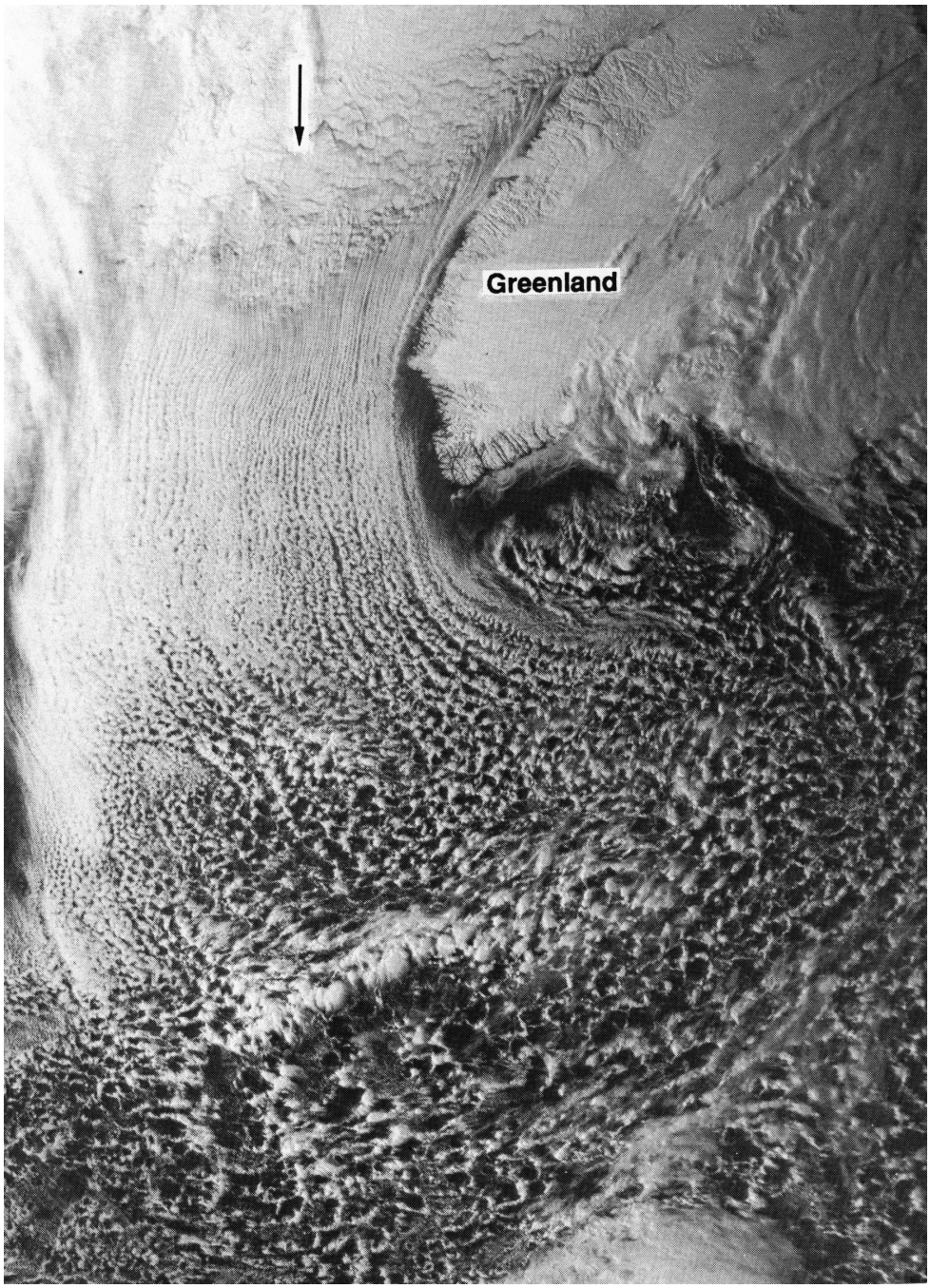

FIGURE 4.2. Satellite (NOAA-7) photograph of the north-east Atlantic ocean and Greenland, made on 19 February, 1984, at 17:03 UT. The arrow indicates the mean wind direction in the convective layer. Courtesy of the University of Dundee.

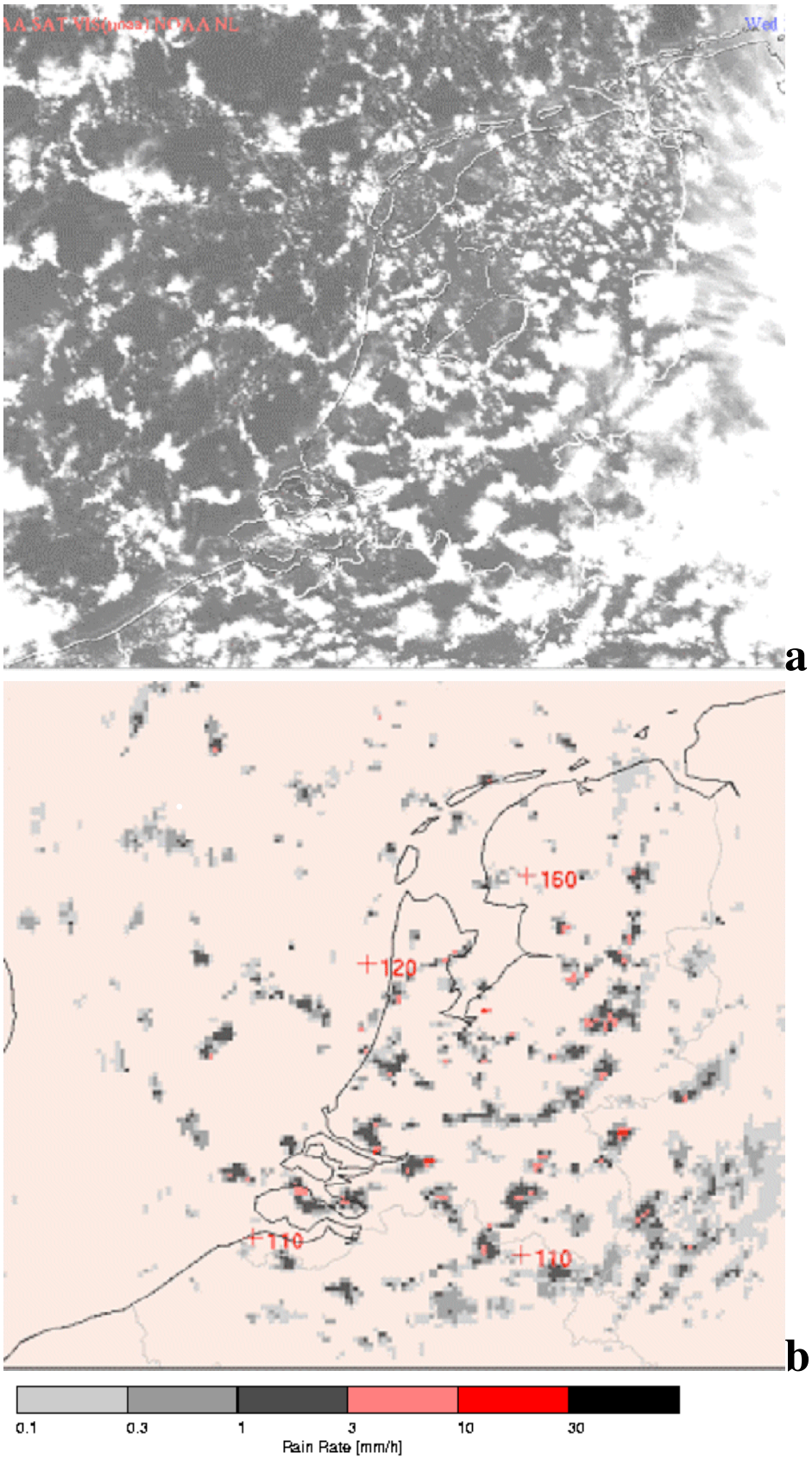

FIGURE 4.3. Panel a: satellite image of open convection cells over the North Sea and the netherlands on April 18, 2001, 12:45 UTC. Panel b: Corresponding radar image displaying precipitation rate and heights (in hundreds of feet; 120 corresponds to about 3500 m) of highest echo (close to the cloud-top). (Figures provided by Ab Maas of KNMI).

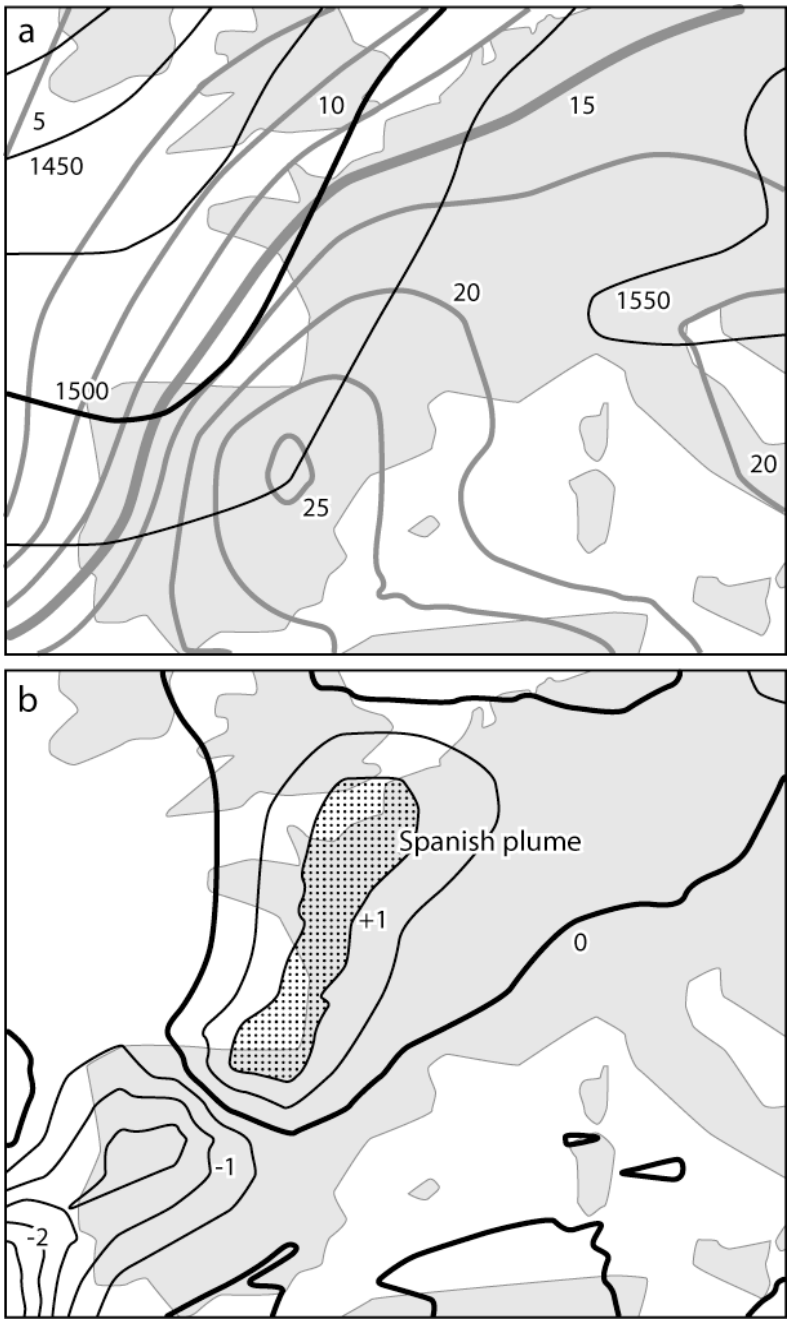

FIGURE 4.4. Height, temperature and temperature advection at 850 hPa on 20 July 1992, 12 UTC. The height, labeled in units of m, and the temperature, labeled in units of °C, are shown in panel (a), while temperature advection , labeled in units of 10^{-4} K s^{-1}, is shown in panel (b).

The subject of atmospheric convection is very complex, especially due to the large effect of phase changes of water (condensation, freezing and evaporation), and due to the presence of hydrometeors (raindrops, snow, graupel and hail stones), which interact in a complicated way with the dynamics. Therefore, the mechanisms behind the organization of cumulus cloud fields are not yet well understood [150].

[150] Atkinson, B.W., and J.Wu Zhang, 1996: Mesoscale shallow convection in the atmosphere. **Reviews of Geophysics**. 34, 403-431.

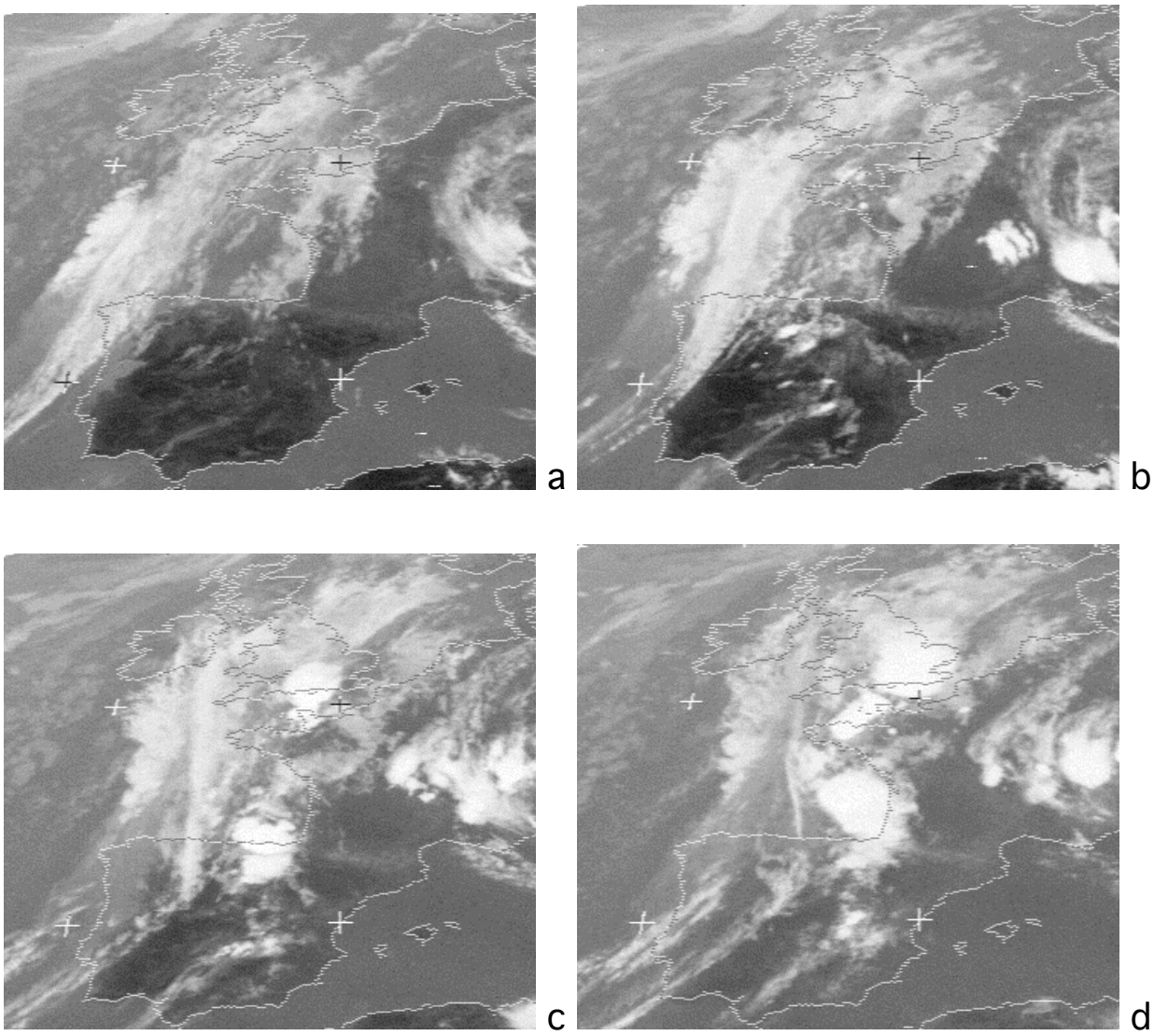

FIGURE 4.5: Meteosat satellite images (infrared channel), 20 July 1992:. (a) 11:30 UTC; (b) 14:30 UTC; (c) 17:30 UTC; (d) 19:30 UTC. Illustration of the outbreak of summer thunderstorms due to forced lifting of potentially unstable air in advance of a cold front over south-west Europe.

4.2 What makes the atmosphere potentially unstable?

Potentially unstable air masses are warm and humid at low levels and cold and dry at upper levels. The atmosphere is **potentially unstable** if the equivalent potential temperature decreases with increasing height (section 1.16). Potential instability may lead to the formation of deep convective clouds, accompanied by lightning and thunder. A potentially unstable stratification of temperature and humidity is created by several factors. The most obvious factor is the heating of the Earth's surface by the Sun, which in turn heats the lowest layers in the atmosphere. Other factors are evaporation of water from the Earth's surface, advection of warm humid air at low levels and advection of cold dry air at upper levels. Advection of warm air at low to mid-levels in the troposphere usually occurs in advance of an approaching cyclone. The atmosphere is destabilized above this warm plume of air, while it is stabilized below. In Western Europe the most famous **warm plume** of this kind is called the "**Spanish plume**" (**figure 4.4**). In the summer half of the year the Spanish plume carries warm and dry air from the boundary layer over the Spanish plateau, which lies at about 1000

m a.s.l., towards the north. When the Spanish plume travels over lower ground (e.g. over western France), it creates a capping inversion at about 1000 m above the Earth's surface. Moisture, evaporated from the Earth's surface into the atmosphere, is stored in the relatively shallow boundary layer beneath this inversion. Above the Spanish plume, at about 3000 m a.s.l., an elevated potentially unstable layer is created. If the moist air in the boundary layer is lifted through the inversion, by some external forcing mechanism, the potential instability is released, leading to an outbreak of severe thunderstorms over France (**figure 4.5**).

4.3 Thunderstorm occurrence related to indications of potential instability

The daily cycle of thunderstorm frequency in De Bilt (about 70 km inland from the Dutch coast) and Vlissingen (at the Dutch coast) over a period of 3 years is shown in **figure 4.6**. The inland station gets more thunderstorms than the coastal station in the afternoon and evening, while the coastal station gets more thunderstorms then the inland station during the night. In the warm season the sea-breeze circulation (section 1.28) plays a role in lifting potentially unstable air over land so that the potential instability, created by Solar heating and surface evaporation, is released. However, over night, when the sea breeze has turned into a land breeze, thunderstorms or showers form over the sea by **forced lifting** of potentially unstable air over the sea in particular in late summer and autumn, when the sea surface is relatively warm. These thundertorms or showers frequently affect the coastal areas.

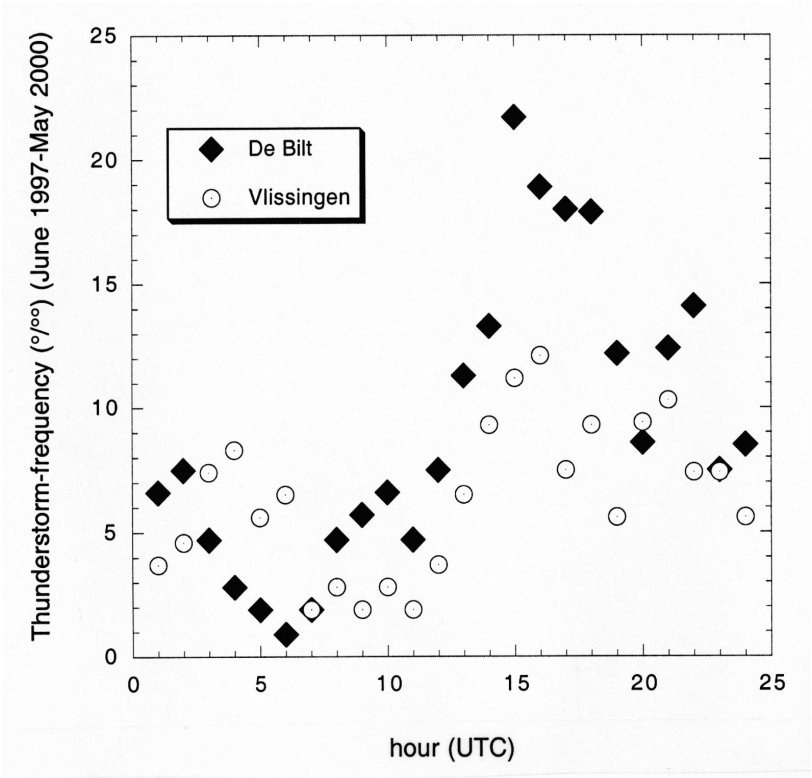

FIGURE 4.6. Thunderstorm-frequency in promille as a function of the time of the day in De Bilt (inland) and in Vlissingen (coast), for the period of time running from June 1, 1997 to May 31, 2000. The thunderstorm-frequency is defined as the total number of thunderstorm reports including precipitation at the time of observation or during the hour prior to the time of observation (ww=17 or 29 or 91-99) divided by the total number of weather reports available at the particular time of observation.

A reasonably good indication of the probability of thunderstorm formation is obtained by evaluating the **Lifted Index**, LI, which is defined as the difference between the observed temperature at 500 hPa and the temperature of an air parcel after it has been lifted pseudo-adiabatically to 500 hPa from its original level. The Lifted Index can be calculated for any sample of air at pressure p>500 hPa if the ambient temperature at 500 hPa is known. Galway (1956)[151] developed the Lifted Index for the prediction of potential instability during afternoon hours by using the forecast maximum temperature near the Earth's surface.

Figure 4.7 gives an impression of the performance of the surface (1.5 m) based Lifted Index as a predictor of summer thunderstorm (i.e lightning) activity in De Bilt. If the lifted index is smaller than -1.5 °C, the probability of lightning occurring within a six hour period after this observation within a circular area with radius of 100 km around the radiosonde launching station (if this is indeed the case then this counts as a "thundery case") is at least 50%. **Figure 4.8** demonstrates that most thundery cases occur if LI<0°C. But this figure also demonstrates that the potential instability (LI<0) in the atmosphere between the surface and 500 hPa is not always released, i.e. many cases with LI<0 are "non-thundery". Probably, these are cases in which potential instability was not be released because of the absence of a dynamical mechanism that can lead to forced lifting of the potentially unstable air and to the release of the potential instability. Conversely, we also observe many thundery cases which are not expected as such, i.e. which are associated with positive lifted index. Probably these are cases where the potential instability is limited to levels well below 500 hPa.

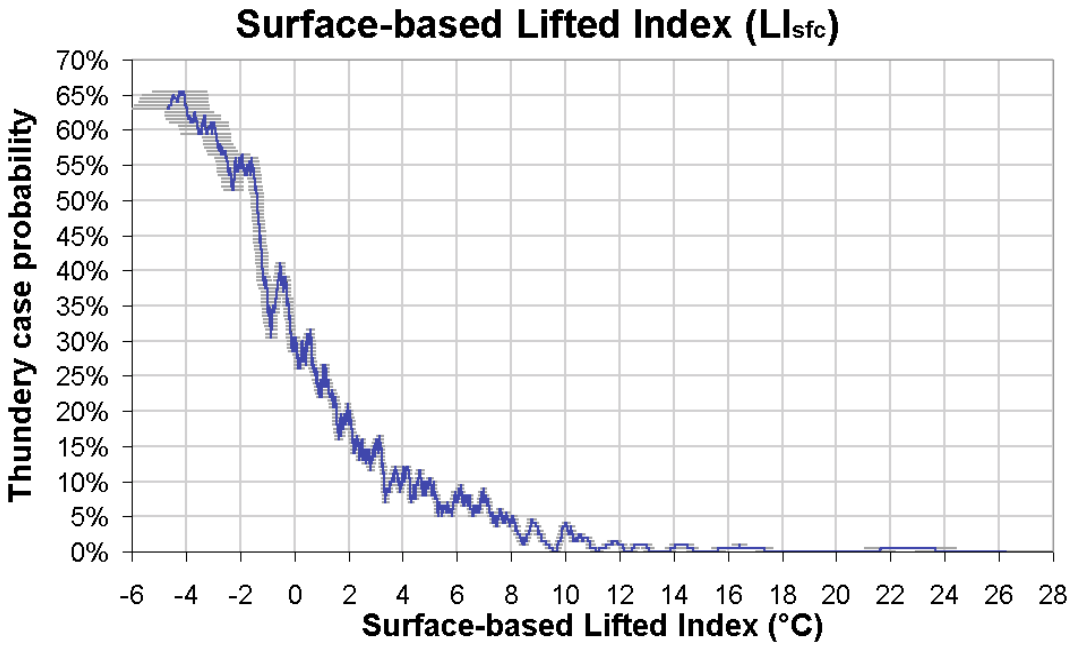

FIGURE 4.7. Thundery case probability (TCP) (including the error bars) as a function of the surface-based Lifted Index for De Bilt (The Netherlands) derived from a data set of consecutive 6-hour intervals spanning a 10-year period. For further details see A. J. Haklander and A. van Delden, 2003: Thunderstorm predictors and their forecast skill for the Netherlands. **Atmospheric Research**, 67-68, 273-299.

[151] Galway, J. G., 1956: The lifted index as a predictor of latent instability. **Bull.Amer.Meteor.Soc**., 37, 528-529.

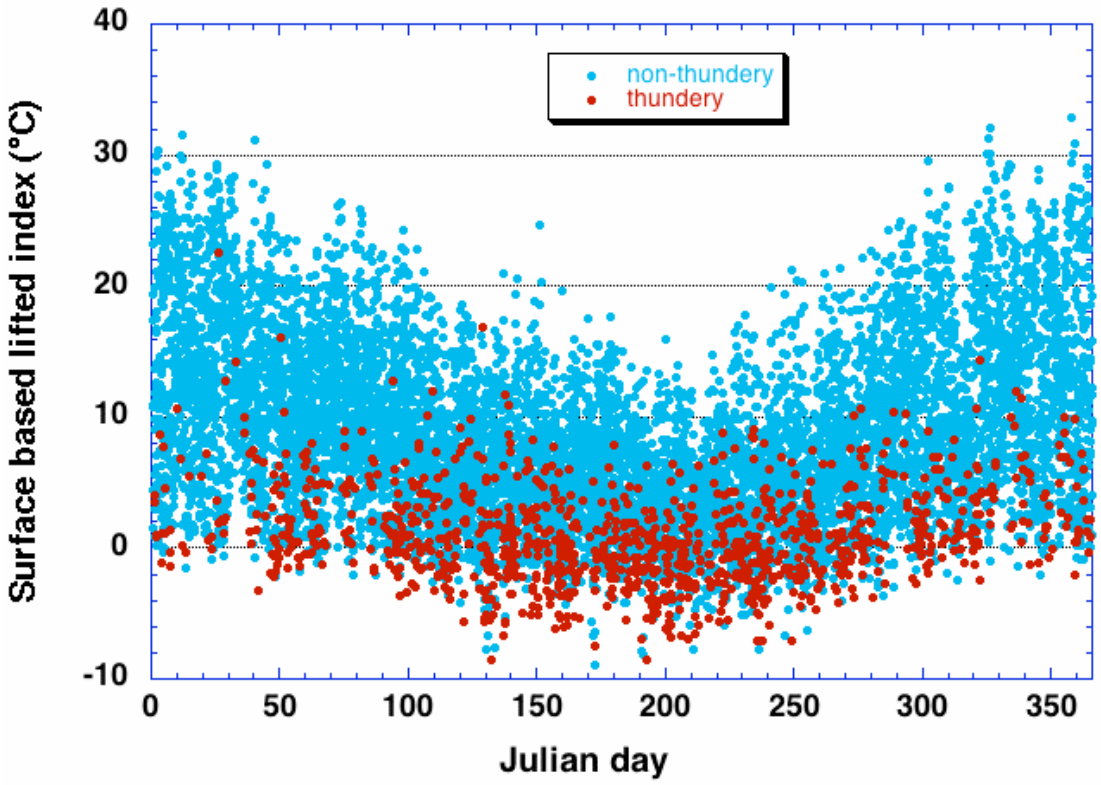

FIGURE 4.8. The dependence of lightning occurrence on the surface based lifted index and the Julian day for 10433 6-hourly intervals within the period January 1990 to June 2000 in the Netherlands. A thundery case is defined as a 6-hour interval within which lightning is detected within 100 km from the radiosonde observation at De Bilt. A 6-hour interval is defined as thundery if lightning is detected within this time interval at less than 100 km from the observation point, where it is understood that the observation is a radiosonde observation at De Bilt launched at the beginning of this time interval. The 1131 thundery cases are indicated by red dots, the 9302 non-thundery cases by cyan dots. A. J. Haklander and A. van Delden, 2003: Thunderstorm predictors and their forecast skill for the Netherlands. **Atmospheric Research**, 67-68, 273-299.

4.4 Forced lifting and release of potential instability

CAPE and LI are measures of the potential for thunderstorm formation in the atmosphere, but these measures do not take into account the role of **forced lifting** in making this potential real. Severe thunderstorms generally only occur if potentially unstable air is lifted in a large area, while moisture is replenishes at low levels by moisture flux convergence. Moreover, large scale forced lifting may destabilize the atmosphere further, as is illustrated in **figure 4.9**. **The intertropical convergence zone (ITCZ) is the most striking permanent zone of forced lifting of potentially unstable air** (**figures 1.12, 1.17, 1.45**). **Mountain slopes are also an obvious source of lift.** The role of mountains in promoting thunderstorms is illustrated by **figure 4.10**, which shows that the greatest thunderstorm frequency in Western Europe is found near the Alpine slopes.

In the middle latitudes an important large-scale source of moisture and lift is provided by a so-called **surface convergence line**, which may attain a length of more than 1000 km over Europe (see e.g. **figures 1.76, 4.11 and 4.12**), and which is usually the footprint at the Earth's surface of a **cross-frontal vertical circulation** (see section 1.33 and chapter 8).

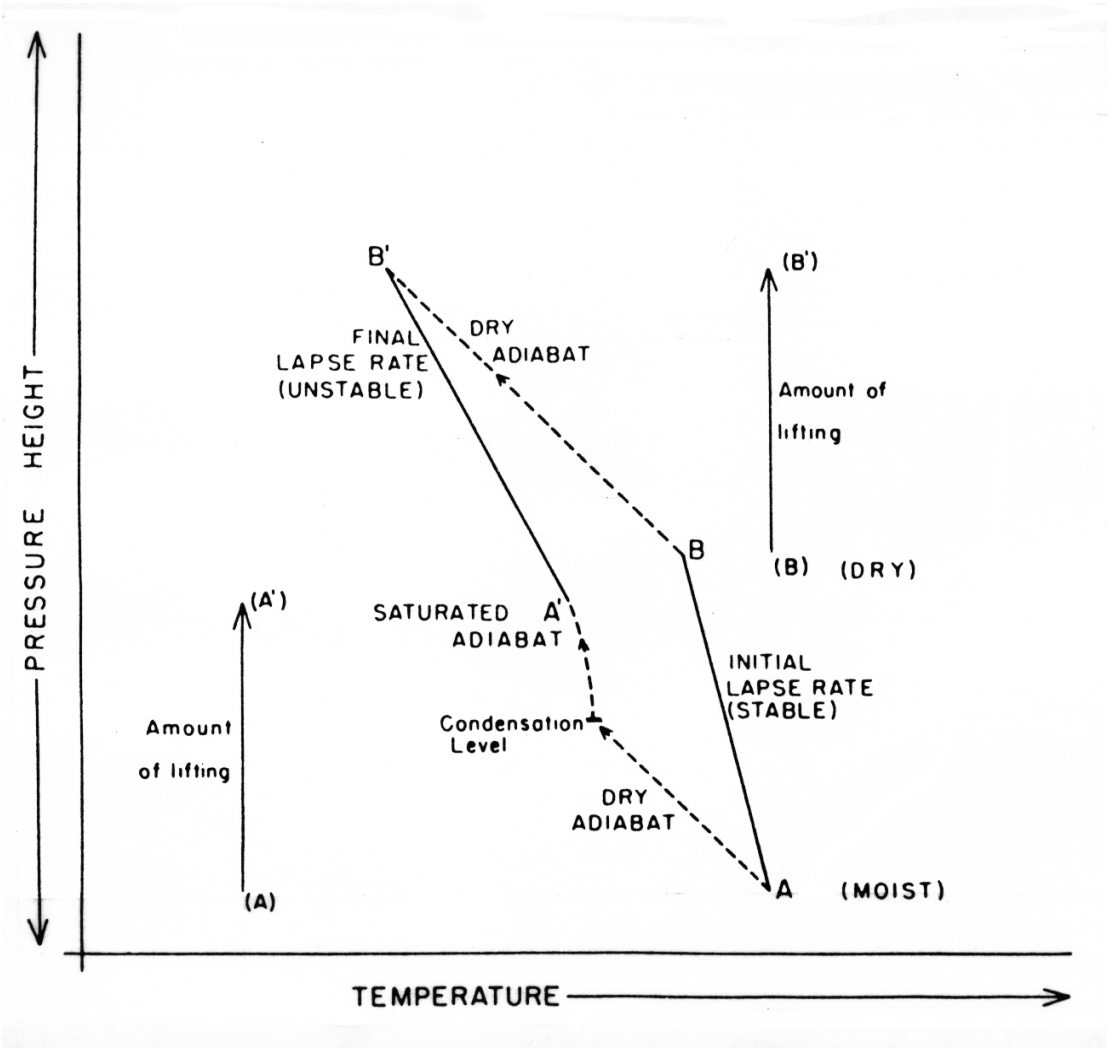

FIGURE 4.9. Potential instability. AB represents the initial state of an column: moist at A, dry at B. After uplift of the whole column the temperature gradient A'B' exceeds the pseudo-adiabatic lapse rate so that the air column is unstable (from: Barry, R.G., and R.M. Chorley, 1987: **Atmosphere, Weather and Climate**. Fifth edition. Methuen, London, 460 pp.).

In late spring and summer in Western Europe the "**Spanish plume**" (**figure 4.4**), which might sometimes be more appropriately called "**African plume**", is instrumental in creating these impressive synoptic features**.** The convergence lines, oberved in **figures 1.76, 4.11 and 4.12**, are the surface manifestation of a secondary circulation which typically accompanies a jetstreak (section 1.35, **figure 1.88**). **Figure 4.13** shows a lower tropospheric jetstreak propagating northward along the western edge of Europe on August 8, 1992. This midtropospheric jetstreak is associated with the intense low-level west-east temperature gradient between the Iberian peninsula and the Atlantic Ocean. **Figure 4.14** demonstrates that the mid tropospheric jet (MTJ), in which the jestreak is embedded, is centred at 5 km above sea-level. The other two jets, labeled ULJ_1 and ULJ_2 in **figure 4.14**, centred at 10 km above sea-level, are associated with an upper-level trough over the Atlantic Ocean (**figure 4.15**). Vertical cross-frontal circulations are required to sustain the accelerations and decelerations of the geostrophic flow in the jetstreak (section 1.35). Systematic forced uplifting is observed in regions of several thousands of square kilometers in connection with these circulations. This large-scale lifing can lead to further destabilization (by the mechanism that is illustrated in **figure 4.9**) and release of potential instability, as also happened on August 8, 1992 (**figure 4.16**).

FIGURE 4.10. Thunderstorm frequency in per mille (as defined in the caption of **figure 4.6**) at more than 200 synoptic weather stations in western Europe for the period April to October of the years 1996-1999 (only observations made at 00, 06, 12, and 18 UTC are used). The frequency is printed in bold if the dataset at the particular station contains more than 3000 observations (at least 88 % of the maximum amount possible), whereas it is printed in plain text if it is based on a series containing between 2000 and 3000 observations. A weather-report is counted as a thunderstorm report if thunder is heard and/or lightning is observed with precipitation one hour before, or at, observation time. The names of several stations mentioned in the text are indicated in the map with the following two-letter abreviations. Ab: Aberporth; Ba: Bastia; Bo: Bordeaux; CF: Clermand Ferrand; DB: De Bilt; Di: Dijon; Ge: Genua; Gr: Grosseto; Gz: Graz; He: Helgoland; In: Innsbruck; Kl: Klagenfurt; Li: Lindenberg; Lo: Locarno; Ly: Lyon; Lz: Lienz; Mi: Milan; Ro: Rome; Si: Sion; sM: St Moritz; Su: Sundsvall; Te: Teruel; To: Toulouse; Tr: Trieste; Tt: Tortosa; Va: Vaduz; Ve: Verona; Za: Zaragoza; Zu:Zurich. Mountain top stations are indicated by one capital letter, i.e. B: Brocken (1142 m); J: Jungfraujoch (3580 m); K: Kahler Asten (834 m); S: Saentis (2490 m) and Z: Zugspitze (2962 m). The frequencies associated with mountain top stations are underlined. Regions 1, 2 and 3 are distinct regions with a high thunderstorm frequency (from Van Delden, A., 2001: The synoptic setting of thunderstorms in western Europe. **Atmospheric Research**, 56, 89-110).

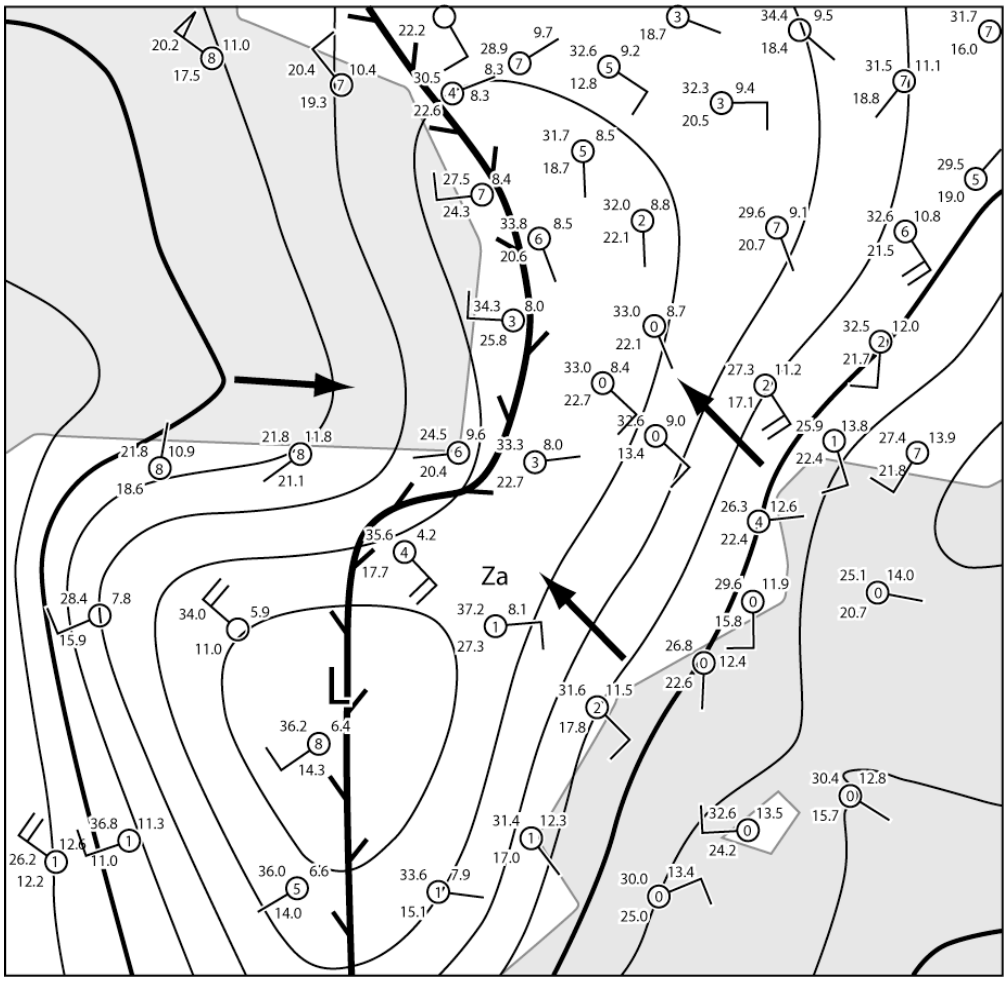

FIGURE 4.11. Surface weather map of 20 July 1992, 15 UTC. The position of a surface station is indicated by a square. The number inside the square indicates the cloudiness (in octas). Also indicated are the temperature (°C) (upper left), the dew point temperature (°C) (lower left) and the pressure (hPa-1000) (upper right). Also shown are sea level isobars drawn every 1 hPa (thick line corresponds to 1012 hPa), according an objective analysis scheme. The letters 'Za" indicate the position of Zaragoza. Arrows indicate the movement and sources of moisture for the thunderstorm. The confluence line is indicated by a "hooked" solid line (from Van Delden, A., 2001: The synoptic setting of thunderstorms in western Europe. **Atmospheric Research**, 56, 89-110). (Compare with fig. 4.5)

A measure of the convergence of mass (including moisture) at convergence lines is provided by **Vertically Integrated Moisture Flux Convergence** (VIMFC) between 1000 hPa and 700 hPa, which is defined mathematically as follows.

$$\mathrm{VIMFC} = -\frac{1}{g}\int_{700\ \mathrm{hPa}}^{1000\ \mathrm{hPa}}\left(\frac{\partial uq}{\partial x}+\frac{\partial uq}{\partial y}\right)dp\,. \qquad (4.1)$$

The distribution of this quantity on a particular day, when severe thunderstorms, accompanied by flash floods, occurred in the Provence (France)[152], is shown in **figure 4.17a**.

[152] Sénési, S., P. Bougeault, J.L. Chèze, P. Cosentino and R. Thépenier 1996: The Vaison-la Romaine Flash Flood: Meso-Scale Analysis and Predictability Issues. **Wea. Forecasting**, **11**, 417-442.

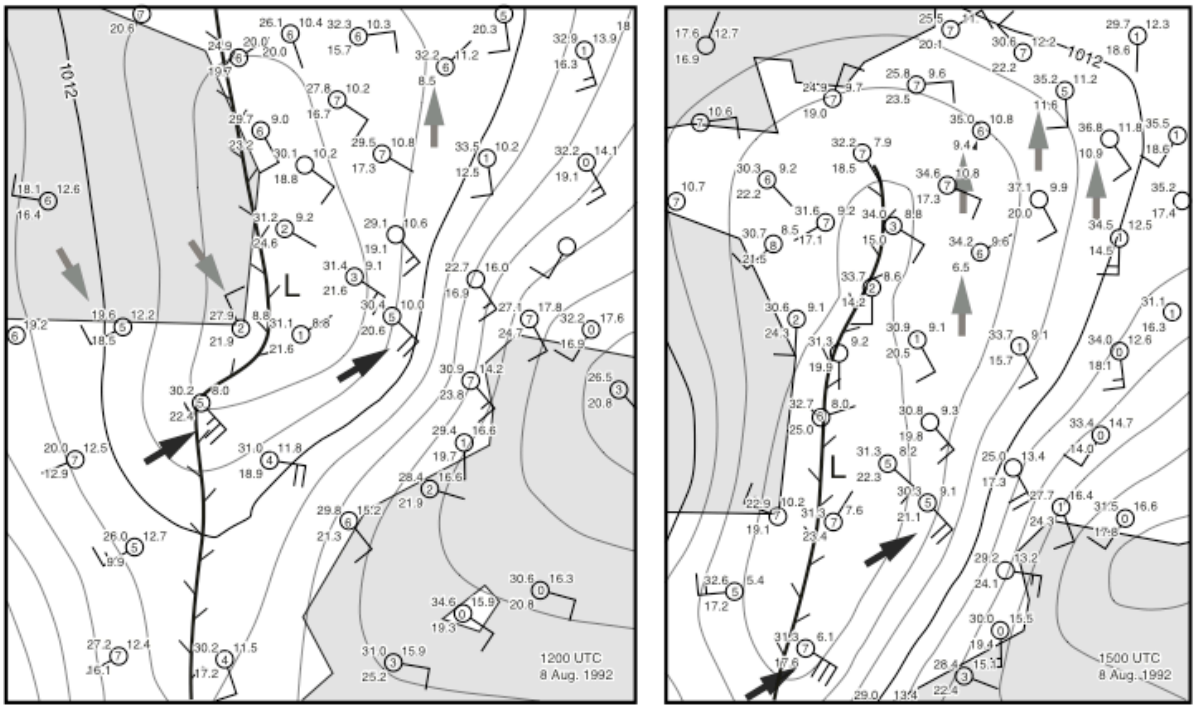

FIGURE 4.12. As **figure 4.11**, but for 8 August 1992, 1200 (left) and 1500 UTC (right). The upward pointing gray arrows highlight the relatively low dewpoints in the north eastern quarter of the "thundery low" (marked by the letter 'L'). The slanting upward pointing black arrows highlight high wind speeds. The slanting downward pointing gray arrows highlight the cool humid air flowing towards the east along the steep north coast of Iberia and the hot, very humid air over south western France.

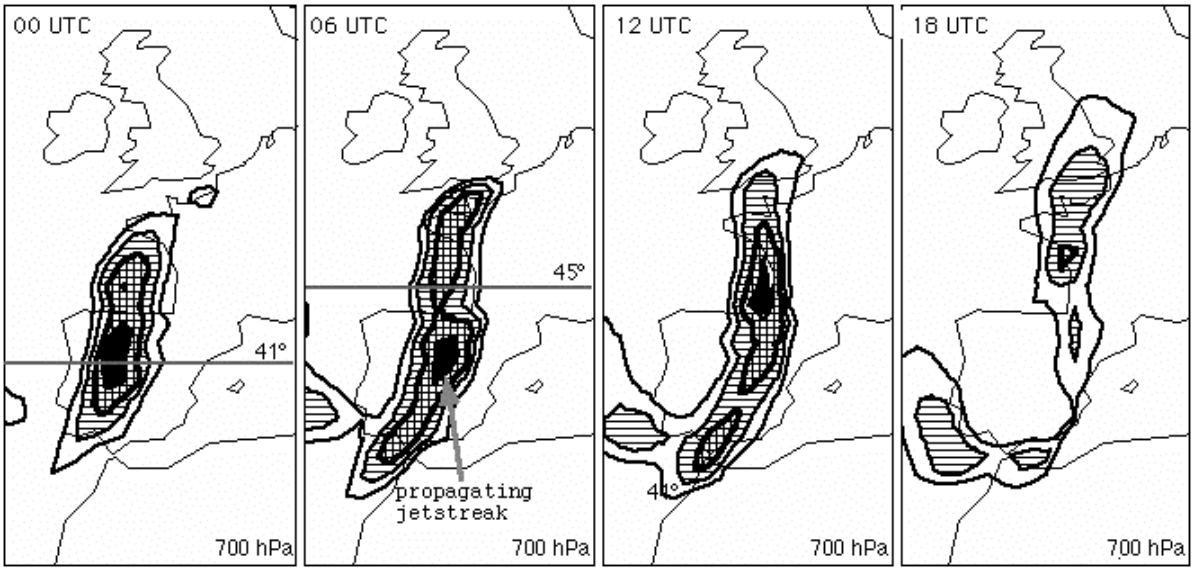

FIGURE 4.13. Absolute windspeed at 700 hPa on 8 August 1992, 0000, 0600, 1200, and 1800 UTC. Isotachs are drawn every 2.5 m/s, starting at 15 m/s. Areas where the windspeed is greater than 22.5 m/s are shaded in black. The jetstreak forms over Iberia and propagates towards the north (ECMWF-analysis).

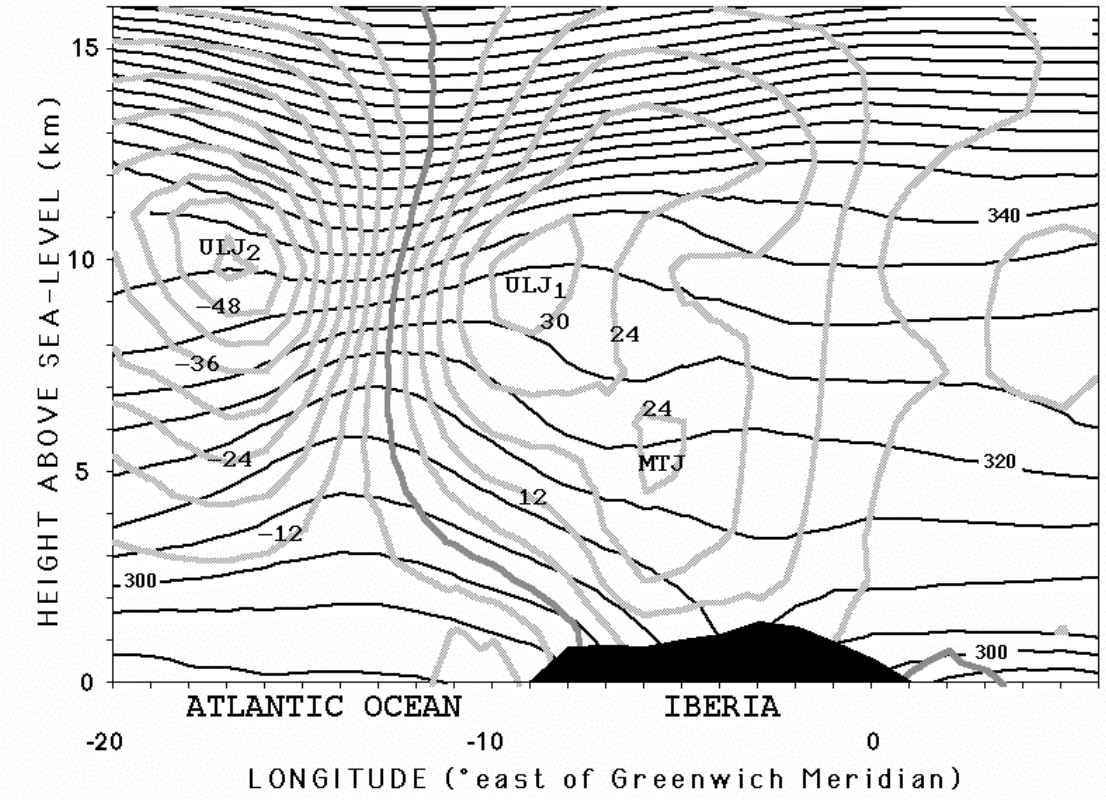

FIGURE 4.14. The potential temperature and the meridional component of the wind velocity as a function of height and longitude for the latitude 41°N (see **figure 4.15**), on August 8, 1992, 0000 UTC, according to the ECMWF analysis. Black lines are isentropes drawn every 5 K. Gray lines are isotachs of the meridional wind (v) drawn every 6 m s^{-1}. The orography of Iberia, smoothed as in the ECMWF analysis/model, is also shown. The jets labeled ULJ1 and ULJ2 are related to the upper level trough. The jet (streak) labeled MTJ is related to an intense low level front over Iberia, which forms due to confluence of hot air originally located over the Iberian plateau and cool air approaching from the Atlantic Ocean (ECMWF-analysis).

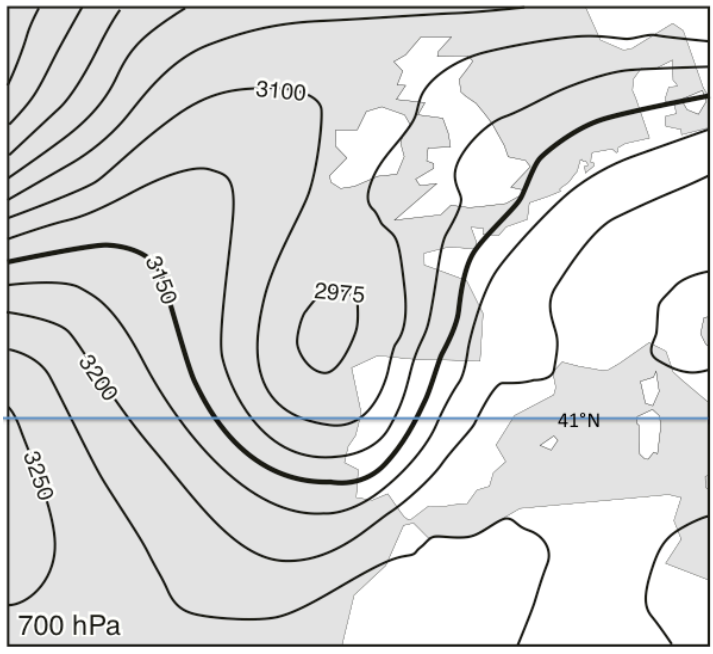

FIGURE 4.15. 700 hPa height, labeled in metres, on August 8 1992, 00 UTC (ECMWF-analysis).

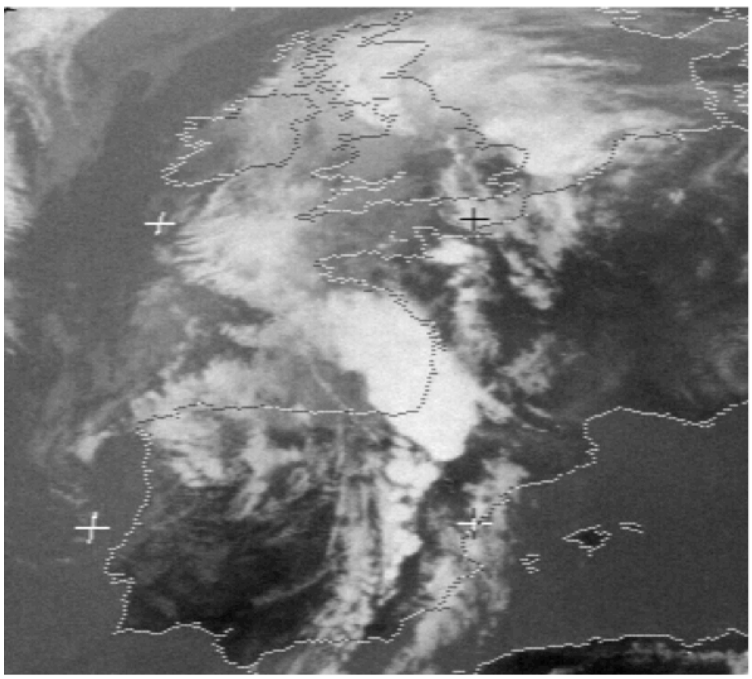

FIGURE 4.16. Meteosat image (infrared) corresponding to Auygust, 8, 1992, 1530 UTC. Many severe thunderstorms arise over the Northern Iberia or South-western France in a south-westerly flow.

Because potential instability is not necessarily released first when air is lifted from the Earth's surface, we now introduce a more general lifted index, which is defined as the temperature at 500 hPa (T_{500}) minus the temperature of a hypothetical air parcel with the characteristics (moisture, temperature and pressure) of its level of origin lifted pseudoadiabatically to 500 hPa, i.e.

$$S_p = T_{500} - T_{p \rightarrow 500} \ , \qquad (4.2)$$

where p represents the pressure of the level of origin of the air parcel, which can be any level below 500 hPa. In (4.2) $T_{p \rightarrow 500}$ is the temperature of a parcel lifted pseudoadiabatically from level p to 500 hPa and T_{500} is the "environmental" temperature at 500 hPa. We subsequently define the **stability of the "most unstable level" (SMUL)** at a particular time and place as the minimum value of S_{1000}, S_{925}, S_{850} and S_{700} at that particular time and place. S_{850} is some times called the "Showalter Index".

During the night the pressure levels 925 hPa, 850 hPa and especially 700 hPa are quite often the "most unstable level". By using the "most unstable level" in the atmosphere as a gauge for the potential of thunderstorms, it is less likely that the formation of nocturnal thunderstorms are overlooked.

Although VIMFC and SMUL are *not* entirely independent of each other, it is nevertheless very interesting to investigate the combination of these two indices as predictor of thunderstorm occurrence. This has been done for the area shown in **figure 4.17**. In the specific case of September 22, 1992 (**figure 4.17**), the most severe thunderstorm activity occurred in the area with both negative values of SMUL *and* large positive values of VIMFC.

Figure 4.18 shows a two-dimensional thundery case probability diagram, valid for summer conditions in Western Europe, excluding mountainous areas. From this diagram it is clear that high positive VIMFC along with negative values of SMUL correlate strongly with the occurrence of thunderstorms.

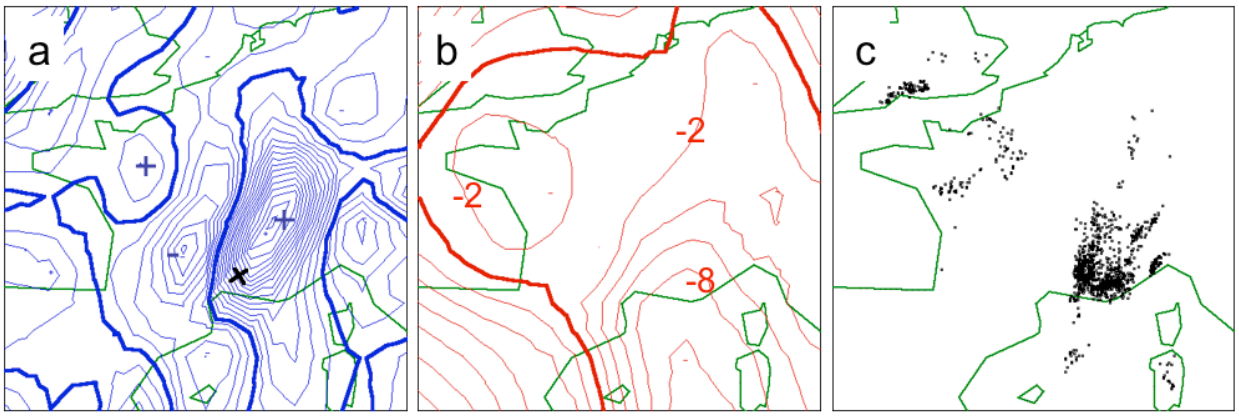

FIGURE 4.17. (a) Distribution of VIMFC over Europe on September 22, 1992, 12 UTC (zero-contour: thick; contour interval is 10 units of 10^{-5} Kg $m^{-2}s^{-1}$). The cross indicates the approximate location of Vaison-La-Romaine. (b) Distribution of SMUL over Europe on September 22, 1992, 12 UTC (zero-contour: thick; contour interval: 2 ˚C). (c) Cloud to ground lightning discharges (black dots) on September 22, 1992, between 12 and 18 UTC fixed by the ATD lightning detection system of the UK Met. Office. **Figures 4.17a and 4.17b** are based on ECMWF-analyses (from J. van Zomeren and A. van Delden, 2007: Vertically integrated moisture flux convergence as a predictor of thunderstorms. **Atmospheric Research**, 83, 435-445).

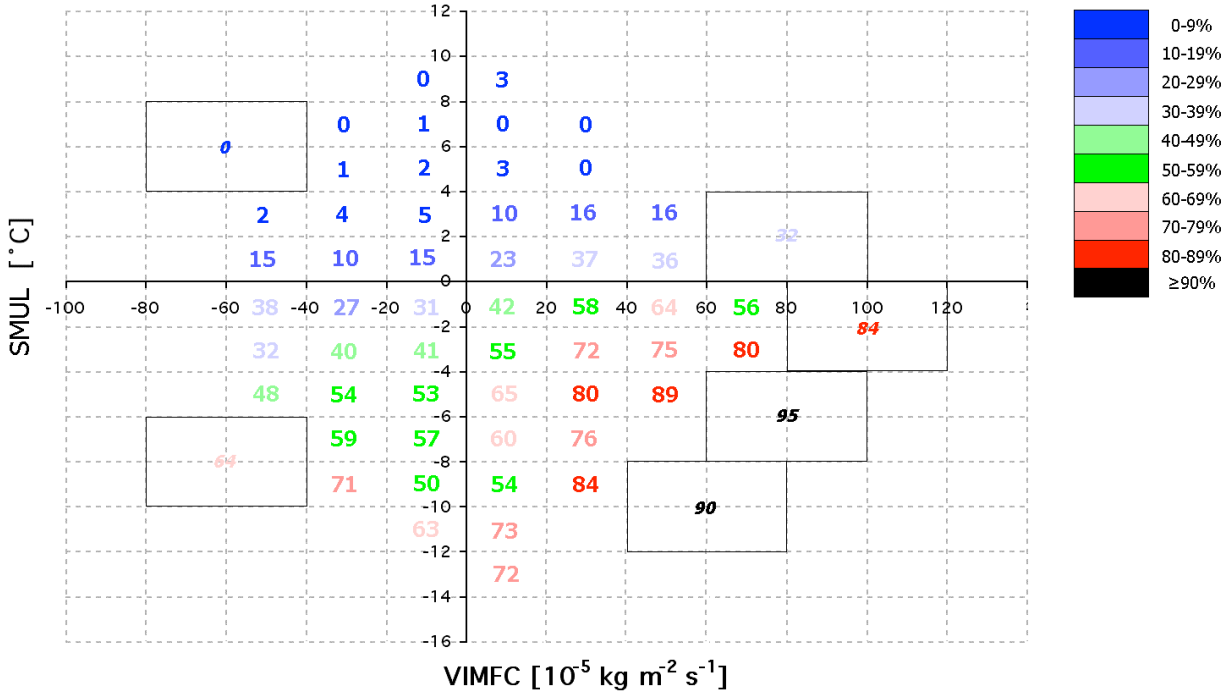

FIGURE 4.18. Thundery case probability (TCP) (defined in **figure 4.8**) as a function of SMUL and VIMFC, valid for summer for an area including the Bay of Biscay, most of France, Southern UK, the English Channel, Benelux, and Northern Germany. TCP per bin (20 units VIMFC (1 unit is 10^{-5} kg m^{-2} s^{-1}) and 2 degrees SMUL) is shown only if there are 25 or more cases. An indication of the thundery case probability in the more rare and extreme cases (see **figure 4.19**) is given in italic by combining four bins if they contain a total of 25 or more cases. The data is based on the gridded operational ECMWF-analyses of two summers (1992 and 1994). The grid distance is 1.5° in latitude and longitude.

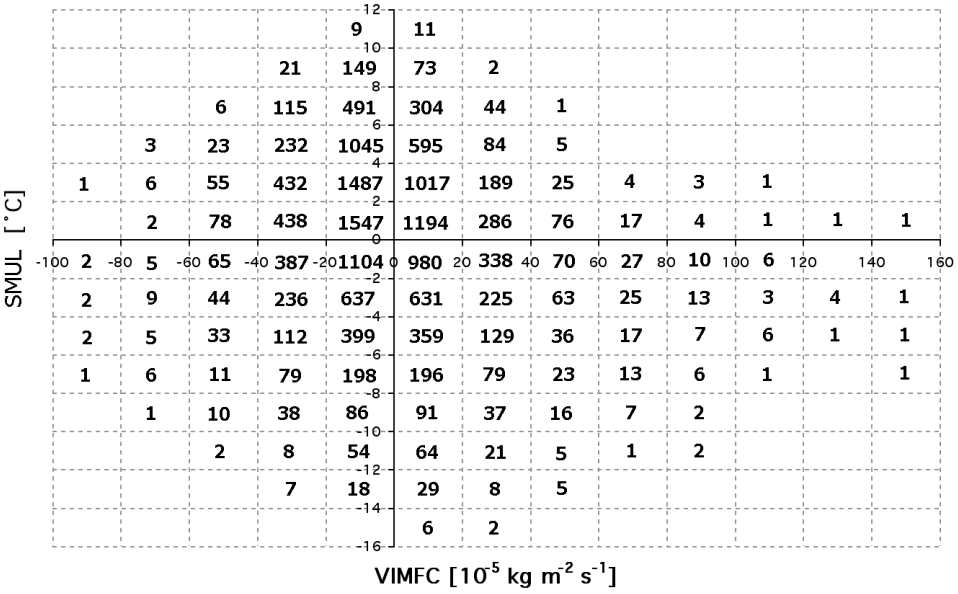

FIGURE 4.19. Distribution of the 17206 cases in parameter (VIMFC and SMUL) space, used for the analysis of **figure 4.18**.

It is important to remember that VIMFC is calculated by taking a mathematical derivative (eq. 4.1), and thus highly dependent on the spatial resolution of the analysis from which it is calculated. Nevertheless, together with the lifted index of the "most unstable level" (SMUL), VIMFC can be very useful as an indicator of the probability of thunderstorm occurrence and it can also be an aid in better pinpointing the location of a possible future thunderstorm.

4.5 Moist convective adjustment

In the lower part of the boundary layer the vertical temperature profile in summer usually adjusts to the dry adiabat due to mixing of air by convection. This process is termed **dry convective adjustment** Above the average height of the lifting condensation level the average stratification tends to adjust quite closely to the moist adiabat. This is noticed most frequently in the upper half of the troposphere, above the average level of maximum heating (at approximately 700 to 500 hPa). This process is termed **moist convective adjustment**.

The idea of convective adjustment has been used frequently in numerical models of the atmospheric circulation in order to represent the effects of convection without explicitly including convection in the model (see e.g. section 2.8). When the computed lapse rate in the model atmosphere exceeds some critical value, the model lapse rate is adjusted back to this critical value, under the assumption of energy conservation. In the case of "dry" convection the critical lapse rate is the dry adiabatic lapse rate (about 10 K km^{-1}). In the case of moist convection, involving phase changes of water, the critical lapse rate is assumed to be the moist adiabatic lapse rate (Box 1.6), whose value is about 6 K km^{-1}. The excess moisture in the layer is assumed to fall out immediately as rain or snow. Hence, the moisture content in the layer is also adjusted under the assumption that the latent heat that is released is converted into internal energy, i.e. leads to a temperature increase.

4.6 The effect of condensed water on buoyancy

In reality condensed water does not fall out of the atmosphere until the liquid water mixing ratio, r_l, has exceeded a certain threshold value. The liquid water present in a moist updraught reduces the upward buoyancy, B, by an amount equal to gr_l. This may significantly reduce the buoyancy force. It may even become negative, in which case the updraught cannot be maintained and the cloud dies out. Liquid water mixing ratios of 0.5 g m^{-3} are not uncommon in ordinary non-precipitating cumulus clouds[153]. As far as its effect on buoyancy is concerned, this is equivalent to a negative temperature perturbation of about 0.15 K if ρ=1 kg m^{-3}. Measurements of total concentration of condensed water at high levels (above 8 km) in severe thunderstorms over Oklahoma of about 10 g m^{-3}, and in one case 44 g m^{-3}, have been reported[154].

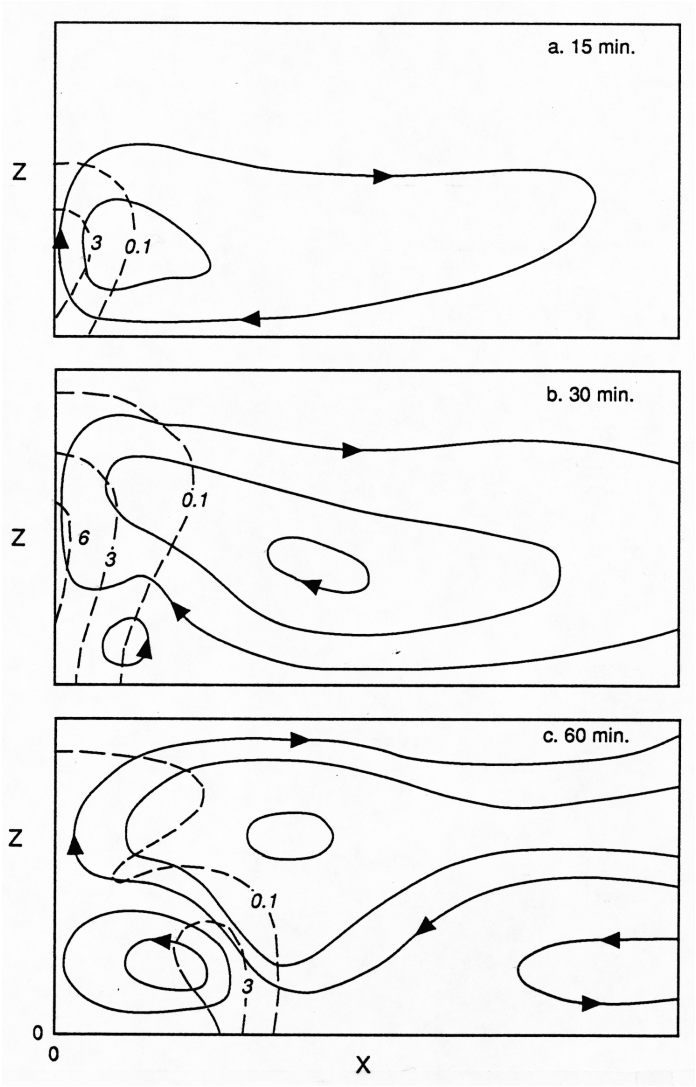

FIGURE 4.20. The streamline pattern (solid lines) in a numerical simulation of an isolated shower. The model is two-dimensional and slab-symmetric around x=0. Rain water content in g m-3 is indicated by dashed lines (from Takeda, T., 1971: Numerical simulation of a precipitating convective cloud: the formation of a "long-lasting" cloud. **J.Atmos.Sci**., 28, 350-376).

---

[153]Rogers, R.R., M.K. Yau, 1989: **A Short Course in Cloud Physics**. Third edition. Pergamon Press, 293 pp.
[154]Ludlam, F.H., 1980: **Clouds and Storms**. Pennsylvania State University Press, University Park, 405 pp.

Except for liquid water loading, as it is called, cooling due to evaporation and melting of falling rain, snow and hail also have a strong influence on buoyancy. In fact, it is estimated that about 20% of the downward acceleration in a strong downdraught (a "**downburst**") and associated **cold pool** of air beneath a thunderstorm cloud is due to condensate loading and 80% is due to cooling as result of melting of snow and hail and evaporation of rain[155].

Obviously, these processes do not promote the maintenance of the updraught or cloud. Numerical model simulations (see **figure 4.20**) have shown that the lower part of the cloud will tend to collapse within one hour. A vertical circulation, with a sign opposite to that of the original circulation, is generated both due to the **"rain water loading"** as well as due to the cooling due to melting and evaporation of precipitation. The updraught associated with this **"cold pool" circulation** is detached from the original updraught. This eventually generates a new cloud beside the old dissipating cloud. Despite this, thunderstorms producing large amounts of rain may persist for many hours. A short discussion of the factors promoting the longaevity of thunderstorms is provided in the following sections.

PROBLEM 4.1. Parcel model of moist convection

This problem is an extension of problem 1.8 to include the effect of release of latent heat due to condensation in an ascending parcel of air. Use the theory described in section 1.16 to extend the model of the buoyancy oscillation of a dry air parcel in a stably stratified environment to an air parcel that contains water vapour. Simulate the vertical movement of such an air parcel in an environment as given in table 1.3. Take account of the fact that condensed water falls out as rain only when the liquid water content of the air parcel exceeds a threshold value. Run the model for different threshold values and consult the literature to find out what a realitic threshold value might be. Does it depend on the vertical velocity?

4.7 Types of Thunderstorms

A buoyantly driven cumulus cloud grows, produces rain and decays over a period of about 1 or 2 hours. These relatively short-lived convective showers are referred to as **"air-mass" thunderstorms**[156]. Since the pioneering study by Byers and Braham it has become ever more clear that more than just a large degree of CAPE is needed to produce a severe thunderstorm that persists much longer than 1 hour. The lifetime of a thunderstorm may be lengthened if the storm is embedded in a large scale flow pattern with vertical wind-shear, with weak wind speeds below and high wind speeds aloft. This configuration allows for a spatial separation of the updraught from the evaporating downdraught and rainshaft, as is shown in **figure 4.21**.

Frequently several thunderstorms, as pictured in **figure 4.21**, are organized in a line perpendicular to the average wind vector. Such a system of thunderstorms is called a **"squall line"**. In the initial stage of the life time of a squall line, this organization is related to the presence of a line surface moisture convergence, as is illustrated in figure 4.12. This effect is referred to the "**synoptic forcing**" of the squall line.

---

[155]Kessinger, C.J., D.B. Parsons and J.W. Wilson, 1988: Observations of a storm containing mesocyclones, downbursts horizontal vortex circulations. **Mon.Wea.Rev.**, 116, 1959-1982.

[156]Byers, H.R., and R.R. Braham, Jr., 1949: **The thunderstorm**. U.S. Govt. Printing Office, 287 pp.

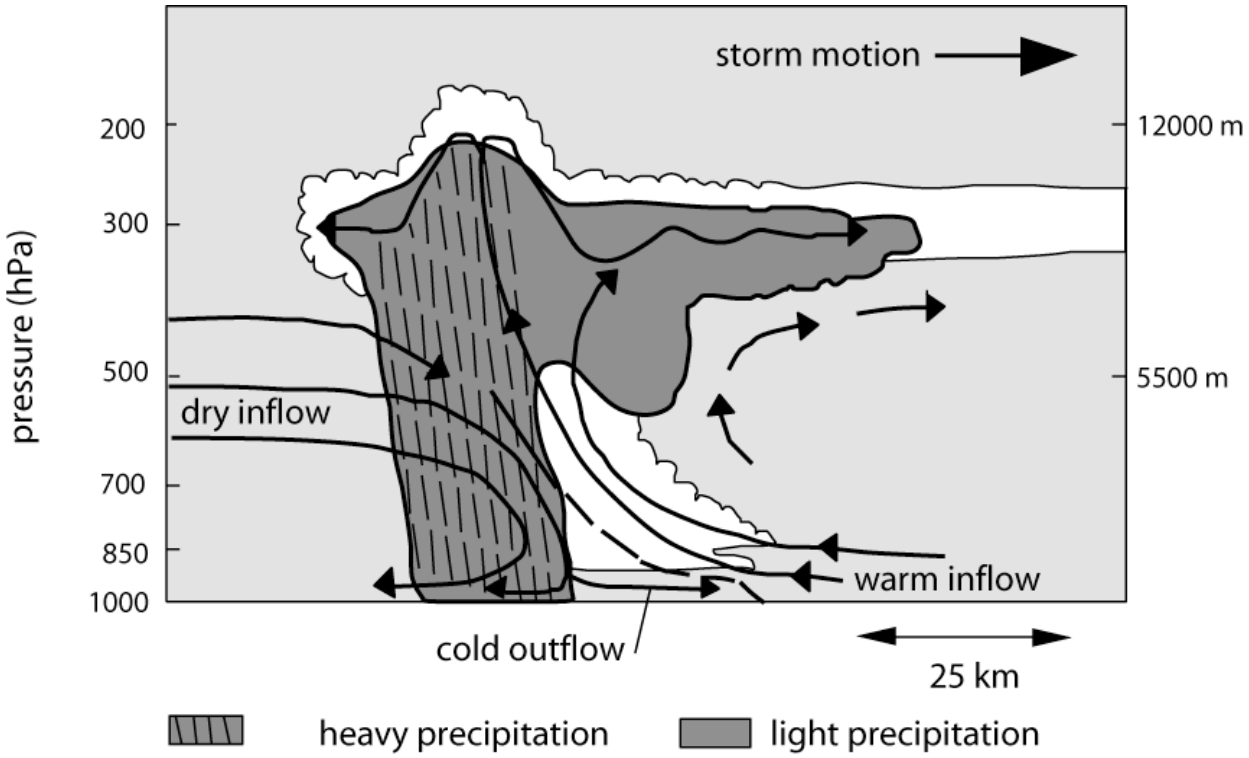

FIGURE 4.21. Cloud boundaries and simplified circulation (arrows denote flow) of a typical mature squall-line-type thunderstorm. Vertical scale has been exagerated fivefold compared with the horizontal scale.

One can, in fact, distinguish several types of thunderstorms, such as, **(a) air-mass thunderstorms, (b) squall lines, (c) multicellular thunderstorms, (d) supercell thunderstorms and (e) meso-scale convective complexes**. In reality this division is not so clear-cut. Most large deep convective weather systems have properties of all five types mentioned above. The convective systems displayed in **figure 1.73** have many properties in common with multicellular thunderstorms and with squall lines.

The type of thunderstorm arrising in a particular environment depends on factors such as large-scale potential instability, vertical shear of the geostrophic wind, forced lifting due to low level convergence or due to orography. The subject is very complicated and, on the theoretical side, it relies heavily on computer simulation. The following sections discuss the most important characteristics of the internal dynamics of severe thunderstorms.

4.8 Interaction of the cold pool with unidirectional shear

The fact that many thunderstorms occur in concert along a line to form a **squall line** allows for a considerable simplification of the theory. As a first and good approximation we can assume that a squall line is a two-dimensional convection cell with clouds organised into a band perpendicular to the mean wind, as is illustrated in **figure 4.21**. A squall line generally moves with a speed greater than the mean wind at lower levels in the troposphere, but slower than the mean wind at higher levels in the troposphere. The level at which the mean wind speed is equal to the propagation speed of the squall line is referred to as the "**steering level**". The height of the steering level of the thunderstorms of July 11, 1984, shown in **figure 1.73**, is about 4 km. Below this level the clouds are fed with warm, relatively humid air from the front side (the right side in **figure 4.21**). Due to the downshear tilt of the

updraught, rain will fall into this inflow stream, which will of course inhibit further storm growth. However, in certain conditions the environmental wind shear can interact constructively with the circulation generated by the cold pool so that the storm can persist and even grow. These conditions were identified first in the 1980's and 1990's with the help of numerical simulations[157]. It was discovered that strong wind-shear in the layer below a height of one or two kilometres above the earth's surface (well below the steering level) and little vertical wind-shear above that layer would produce the most long-lived storms. This represents the "optimal state" for long-lived squall lines. The absence of wind shear above the steering level prevents the storm from leaning downshear and reduces the inhibiting effect of shear on the updraught. The effect of the low level relative countercurrent with shear is subtle. The cold pool circulation and the circulation associated with the low level shear in the optimal state have opposite signs. This is favourable for the maintainance of the updraught and also keeps the updraught in place relative to the storm.

PROBLEM 4.2. **Thermodynamic conditions during the passage of two squall lines over De Bilt on July 11, 1984 (figures 1.73-1.76)**
Estimate the height of the steering level of the squall lines that passed over the Netherlands on July 11, 1984 from the radiosonde observations at De Bilt (http://weather.uwyo.edu/upperair/sounding.html).

4.9 Thunderstorm splitting and formation of tornadoes

In unidirectional shear, conditions for long-lived convective storms, where the storm maintains its identity as a line of clouds oriented perpendicular to the environmental wind, are not easily fulfilled. The "rain-water loading" effect will usually induce a **splitting** of the updraught as shown in **figure 4.22**. Radar observations of thunderstorm splitting over the Netherlands are shown in **figure 4.23**.

After the splitting of the updraught, two new counter-rotating updraughts are formed, which travel to the right and left of the original convective storm. This can be understood with the help of a linearised vertical vorticity equation. To obtain this equation, we simplify matters by neglecting friction, diabatic heating and Earth's rotation. We assume that dynamic state of the atmosphere can be split into a hydrostatic reference state, characterized by a steady wind $u_0(z)$, and a perturbation of this reference state. We thus assume that $u=u_0(z)+u'(x,y,z,t)$ and likewise for Π and θ, where $u'<<u_0$, $\Pi'<<\Pi_0$, $\theta'<<\theta_0$ and $\partial\Pi_0/\partial z = -g/\theta_0$. The primes, that are attached to u, θ and Π, indicate perturbations relative to the hydrostatic reference state. We further simplify matters by assuming that $\theta_0 = \theta_m$ = constant (eq. 3.2). This is in fact the shallow Boussinesq approximation (section 3.2). Strictly speaking, we cannot apply this approximation to deep convection. However, we are not aiming for exact quantative results, but only aim to identify the basic mechanisms associated with the interaction of convection with vertical shear of the large scale wind.

---

[157]Thorpe, A.J. and M.J. Miller, 1978: Numerical simulations showing the role of the downdraught in cumulonimbus motion and splitting. **Q.J.R.Meteorol.Soc.**, 104, 873-893.
Rotunno, R., J.B. Klemp and M.L. Weisman, 1988: A theory for strong, long-lived squall lines. **J.Atmos.Sci**., 45, 463-485.
Weisman, M.L. and R. Rotunno, 2000: The use of vertical wind shear versus helicity in interpreting supercell dynamics. **J.Atmos.Sci.**, 57, 1452-1472.

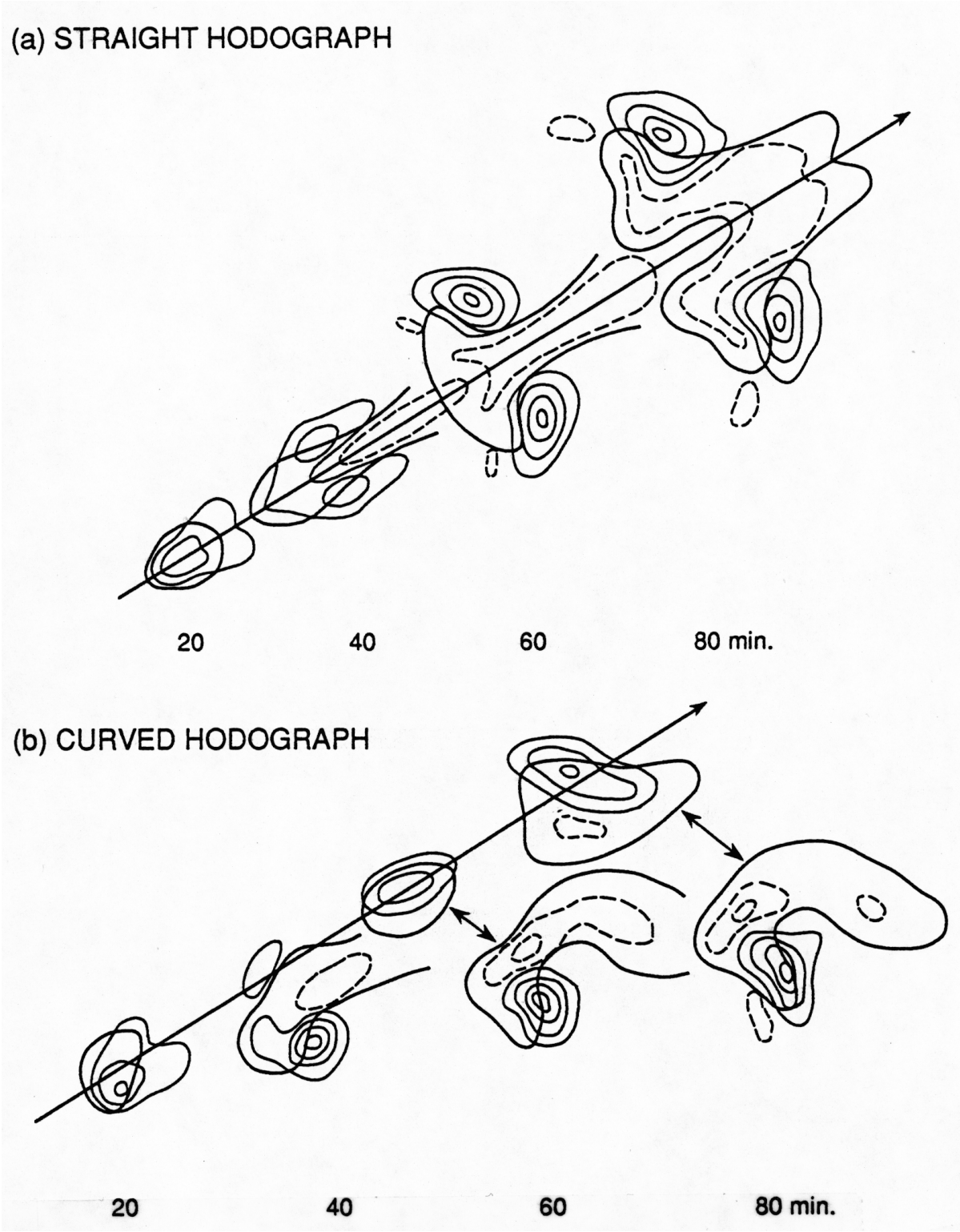

FIGURE 4.22. Horizontal contour plots of vertical velocity at 2.25 km above ground level at different times in a numerical simulation with the three-dimensional cloud model described by Klemp and Wilhelmson (1978) for two cases: (a) with an environmental wind which increases in speed but not in direction with increasing height, and (b) with an environmental wind which increases in speed and veers clockwise with increasing height. Updraughts (solid lines) and downdraughts (dashed lines) are contoured at 4 m s^{-1} increments. The heavy line is the outline of the 0.5 g m-3 rainwater field (from Rotunno, R. and J.B. Klemp, 1982: The influence of the shear-induced pressure gradient on thunderstorm motion. *Mon.Wea.Rev.*, 110, 136-151.

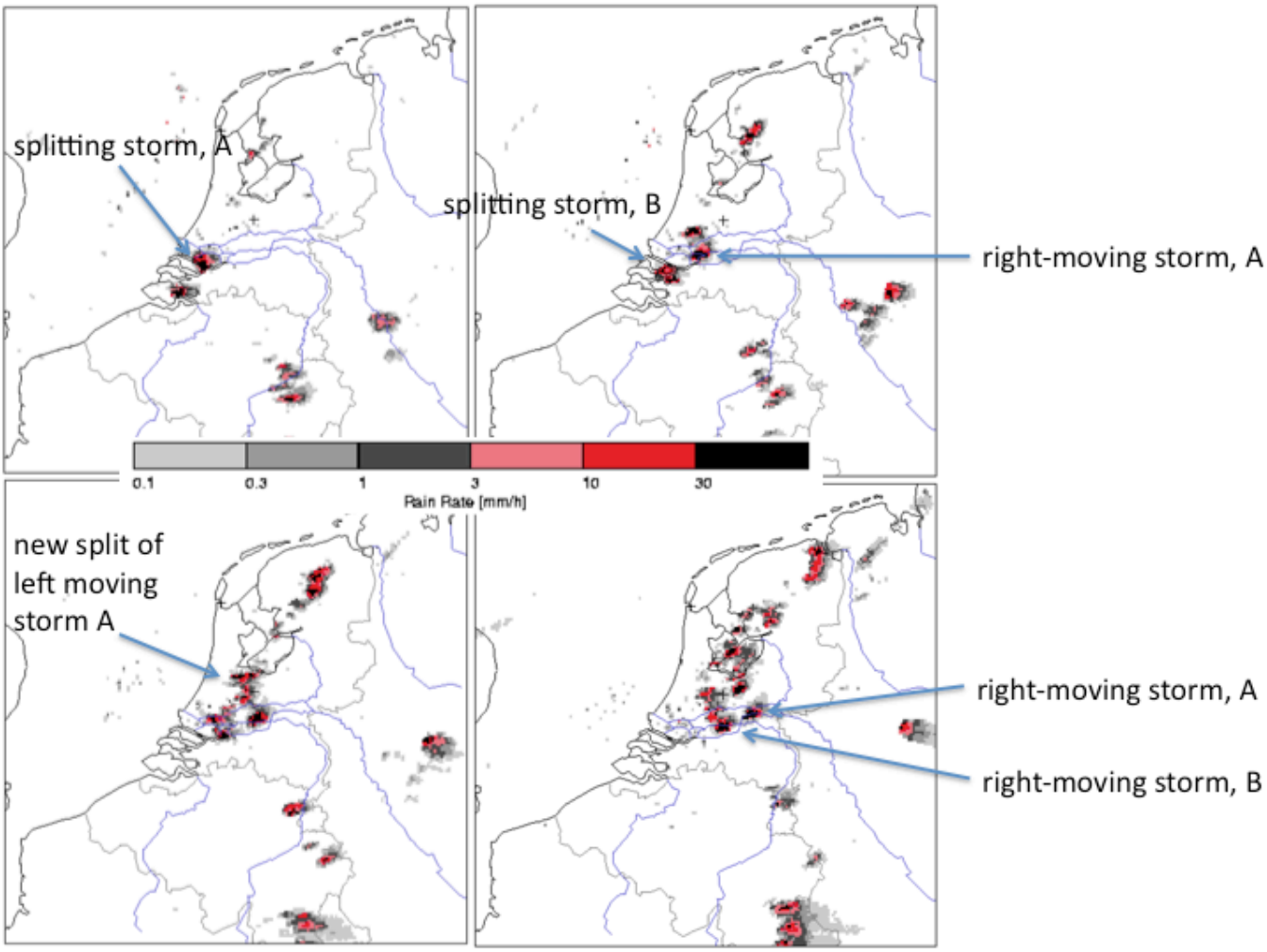

FIGURE 4.23. Radar-echo's (i.e. precipitation intensity) maps corresponding to July 21, 1995, for 4 consecutive times (at half hour intervals), showing the splitting of small thunderstorms over the Netherlands, where the right moving storm attains the greatest rain rate. Upper left: 1715 UTC; upper right: 1745 UTC; lower left: 1815 UTC; lower right: 1845 UTC. (Thanks to Marco Verhoef and Sander Tijm, KNMI, De Bilt.)

The three components of the momentum equation 1.56 (see also eqs. 3.6a-c) linearized around the reference state, become,

$$\left(\frac{\partial}{\partial t}+u_0\frac{\partial}{\partial x}\right)u \equiv G(u) = -\theta_m\frac{\partial \Pi}{\partial x} - w\frac{\partial u_0}{\partial z}\ , \tag{4.3}$$

$$\left(\frac{\partial}{\partial t}+u_0\frac{\partial}{\partial x}\right)v \equiv G(v) = -\theta_m\frac{\partial \Pi}{\partial y}\ , \tag{4.4}$$

$$\left(\frac{\partial}{\partial t}+u_0\frac{\partial}{\partial x}\right)w \equiv G(w) = -\theta_m\frac{\partial \Pi}{\partial z} + \frac{\theta}{\theta_m}g\ , \tag{4.5}$$

where the primes, which are attached to u, θ and Π, have been dropped. An equation for the vertical component of the relative vorticity, ζ $(=\partial v/\partial x - \partial u/\partial y)$, is easily obtained from eqs.(4.3) and (4.4). This yields

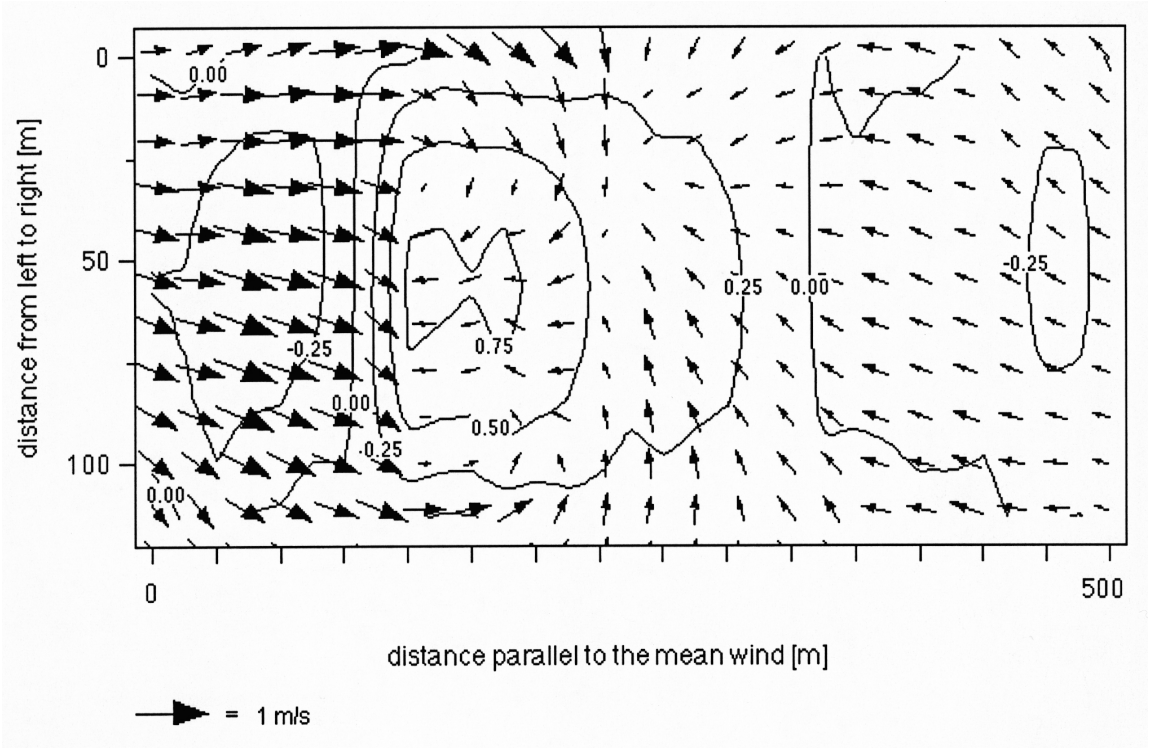

FIGURE 4.24: Measured horizontal wind field, relative to the mean wind, corresponding to the average convective updraught in vertically sheared flow in the atmospheric surface layer at 13 m above the earth's surface in statically unstable conditions. Contours are the vertical velocity in m s^{-1}. The mean wind is directed parallel to the *x*-axis. (from Weijers, E.P., A. van Delden, H.F. Vugts and A.G.C.A. Meesters, 1995: The composite horizontal wind field within convective structures of the atmospheric surface layer. **J.Atmos.Sci.**, **52**, 3866-3878).

$$G(\zeta) = \frac{du_0}{dz}\frac{\partial w}{\partial y} \quad . \tag{4.6}$$

The operator, G, is defined in the equations above. Equation 4.6 expresses the approximate material time rate of change of ζ due to tilting to the vertical of horizontal environmental relative vorticity due to horizontal shear of the vertical velocity. The most intense rotation around the vertical axis is thus created at the flanks of the updraught. If the mean wind speed increases with increasing height, i.e. $du_0/dz>0$, eq. 4.6 states that ζ will be positive if $\partial w/\partial y>0$, which is the case on the right flank of the original updraught. Therefore, the right moving updraught acquires positive vertical relative vorticity (in the northern hemisphere this corresponds to counter-clockwise rotation), whereas the left moving updraught acquires negative vertical relative vorticity. This is confirmed on a smaller scale by measurements around convective updraughts within the surface layer of the atmosphere (**figure 4.24**).

The interaction of the updraught with the environmental shear creates **dynamic pressure perturbations** below and in the clouds. This can be understood from the linear diagnostic equations (4.3-4.5)[158]. If we differentiate (4.3) with respect to x, (4.4) with respect to y and (4.5) with respect to z and add the results, using the "shallow Boussinesq approximation" of the continuity equation (3.14), and assuming a linear dependence of u_0 on height, z, we

[158] Rotunno, R. and J.B. Klemp, 1982: The influence of the shear-induced pressure gradient on thunderstorm motion. **Mon.Wea.Rev.**, 110, 136-151.

obtain a Poisson equation for the Exner function:

$$\theta_m \nabla^2 \Pi = -2 \frac{du_0}{dz} \frac{\partial w}{\partial x} + \frac{g}{\theta_m} \frac{\partial \theta}{\partial z}. \qquad (4.7)$$

The Exner function,

$$\Pi \equiv c_p \left(\frac{p}{p_{ref}} \right)^{\kappa}$$

is defined first in eq. 1.53.

Equation 4.7 shows that Π (or p) is determined by shear as well as by stratification or buoyancy. Pressure perturbations, resulting from the interaction of updraught or downdraught with the mean vertical shear, are termed "**dynamic**", while the pressure perturbations resulting from buoyancy are termed "**static**". Aircraft-measurements of the perturbation pressure field around the cloud-base of convective clouds due to LeMone et al.[159] show that the pressure perturbation variations in and around these clouds are principally "dynamically" induced. Pressure perturbation extrema measured in deep sheared cumulus clouds were typically 1 hPa, with a range from 0.2 to 9.5 hPa. In contrast, in shallow clouds with little wind shear the extrema are in the order of 0.1 hPa.

Dynamic pressure perturbations in thunderstorms play an extremely important role in organizing the convective storm and possibly exiting tornadoes. Thjis can be qualitatively understood from eq. 4.7, which, neglecting buoyancy and stratification, simply becomes

$$\theta_m \nabla^2 \Pi = -2 \frac{du_0}{dz} \frac{\partial w}{\partial x}$$

If we assume that Π can be written as $A\exp\{i(kx+nz)\}$, we can easily deduce that $\nabla^2\Pi \approx -\Pi$. This implies that the above linear equation can be approximated by

$$\Pi \approx \frac{2}{\theta_m} \frac{du_0}{dz} \frac{\partial w}{\partial x}. \qquad (4.8)$$

From this equation we see that, if $du_0/dz>0$, Π will be positive on the **upshear** side of the updraught, where $\partial w/\partial x>0$, while Π will be negative on the **downshear** side, where $\partial w/\partial x<0$. This leads to a **negative vertical pressure gradient on the downshear side, which promotes updraught propagation downshear**. However, if the background wind, u_0, does not turn with height, the updraught is still strongly inhibited by the "rain-water loading effect" (section 4.6).

The "dynamic" pressure gradients do, however, play an important role in thunderstorm dynamics when the environmental wind turns with height. Most cases of deep convection in the Northern hemisphere, such as in North America and in Europe, are associated with advection of warm air. Under these circumstances, the wind-direction turns clockwise

---

[159] Le Mone, M.A., J.C. Frankhauser, G.M. Barnes and L.F. Tarleton, 1988: Perturbation pressure fields measured by aircraft around the cloud base updraft of deep convective clouds. **Mon.Wea.Rev., 116**, 313-327. Le Mone, M.A., J.C. Frankhauser and G.M. Barnes, 1988: Perturbation pressure fields at the base of cumulus clouds in low shear. **Mon.Wea.Rev., 116**, 2062-2068.

(veers) with increasing height (section 1.31). This induces the strongest negative *vertical* dynamic pressure gradient on the downshear side of the right-moving storm (looking the direction of propagation of the storm), because the background wind shear in the direction of storm propagation is largest for the right moving storm. This in turn favours the growth of the right-moving updraught (**figures 4.22b**). With very intense vertical shear (strong horizontal temperature gradients) coupled to strong veering of the background wind with height (intense warm air advection), the counter-clockwise rotating right-moving storm may turn into a so-called **"supercell thunderstorm"**, which is the most violent type of thunderstorm (see **figure 4.25**).

The rotation and the dynamically induced vertical pressure gradient may cooperate to produce tornadoes. The question how exactly this works, is interesting but beside the scope of this text (see the book by Paul Markovski and Yvette Richardson[160] for more information on these interesting dynamical phenomena).

Supercell storms occur most frequently in the southern interior states of North America, to the east of the Rocky mountains, where high levels of potential instability frequently are coupled to intense large scale warm air advection from the Gulf of Mexico, in particular in Spring. They also occur less frequently in other parts of the world where these circumstances occur, such as in Western Europe in the months of May to August, in South America (in particular Northern Argentina) and in Southern China.

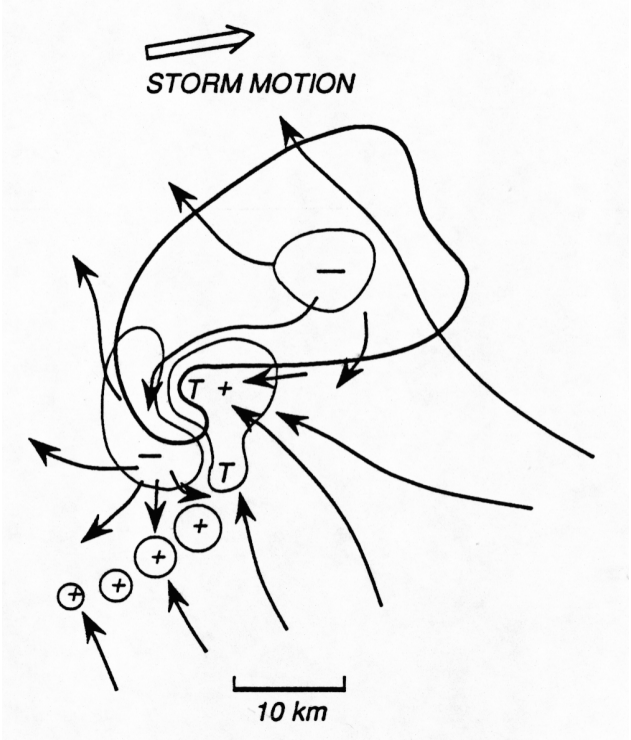

FIGURE 4.25. Schematic plan of a tornadic supercell thunderstorm. The solid line encompasses the radar echo, indicating precipitation. Regions with strong vertical motion are enclosed by thin solid lines and marked with a plus sign (upward motion) or a minus sign (downward motion). The flow near the ground is indicated by arrows. Tornadoes are most likely to form at the points marked by a 'T'. Recently this type of storm has been simulated numerically at very high resolution of 30 m in all directions, the results of which have been presented at a conference in November 2014 (see https://www.youtube.com/watch?v=1JC79gzZykU).

[160] Markowski, P.M., and Y.P. Richardson, 2010: **Mesoscale Meteorology in Midlatitudes**. John Wiley, 430 pp. (sections 8.4 and 10.1).

PROBLEM 4.3. **Thermodynamic conditions during the passage of the splitting thunderstorms on July 21, 1995 (figure 4.23)**
Analyse the conditions in the environment of the splitting thunderstorms of July 21, 1995 over the Netherlands using radiosonde measurements downloaded from http://weather.uwyo.edu/upperair/sounding.html. Do you expect the preferred growth of the right-moving storms?

4.10 The meso-scale convective complex

Finally, we discuss very shortly a type of convective weather system, which does not require large environmental vertical wind-shear. It is termed **Meso-scale Convective Complex** (MCC). The MCC, which was identified first by Maddox[161], has a more circular form than a squall line (at least on satellite images) and travels relatively slowly. It has a relatively long lifetime (>12 hours), acquires a large areal extent (>10^5 km^2) and produces tremendous amounts of rain at one location. MCCs result from mergers and interactions between groups of storms that develop in different locations. Some MCCs are initially squall lines that acquire MCC-characteristics. Presumably large-scale low-level convergence induced by, for example, a slowly moving cold core upper level cyclone, keeps these systems going. Orographic lifting may also contribute to the long lifetime. Due to the slow movement of the MCC and its long lifetime, prolonged and intense latent heating occurs in the middle of the troposphere. In the later stages of the lifetime of an MCC, a cyclonic warm-core vortex appears at mid-levels. At higher levels, an anticyclonic circulation develops. The cyclonic circulation at mid-levels can frequently be seen in the cloud pattern of decaying MCCs on satellite images. MCCs have many features in common with tropical cloud clusters and with torrential rainstorms occurring in the autumn over the warm Mediterranean Sea and adjacent coast frequently also in connexion with a large scale cold-core cyclone.

FIGURE 4.26. A **shelf cloud** near Titz in Germany, half way between Monchengladbach and Aachen (near the border with the Dutch province of Limburg) at 18:30 UTC on 9 June 2014. The shelf cloud formed ahead of a severe thunderstorm. Cold downdraft air surges out along the surface and lifts the warm air ahead of the storm up to condensation level (see **figure 4.21**). A smooth shelf-like cloud forms, skirting the thunderstorm. The shelf cloud is usually accompanied by a gustfront. This image is due to Michiel Baatsen.

[161]Maddox, R.A., 1980: Mesoscale convective complexes. **Bull.Amer.Meteor.Soc**, 61, 1374-1387.

ABSTRACT OF CHAPTER 4

Boundary layer shallow convection is a common phenomenon in the atmosphere of the Earth. It occurs in particular on summer days when the Sun heats the Earth, giving rise to surface layer instability It occurs also over the ocean in cold air outbreaks.

Deep convection in the free atmosphere (above the boundary layer) with clouds tops reaching the upper troposphere is a less common phenomenon. Large values of CAPE (Convective Available Potential Energy) are required. In fact, occurrence of lightning (a measure of thunderstorm occurrence) correlates better with the **Lifted Index** (LI) than with CAPE.

But despite intense potential instability (i.e. large values of CAPE or large negative values of LI), deep convection usually does **not** occur spontaneously. "**Forced lifting**" and associated **moisture flux convergence** are required to release and replenish the potential instability. The synoptic features causing the forced lifting are, for instance, mountain slopes and mid-tropospheric jetstreaks. Mid-tropospheric jetstreaks are connected to low-level frontogenesis. The important topic of forced lifting is addressed in more detail in chapters 8 and 9.

A very short introduction is given into the complex dynamics of deep, severe convective thunderstorms. Processes discussed are **water loading**, **thunderstorm splitting** and the role of the **vertical shear of the mean wind** in promoting the lifetime of a precipitating cloud. Also discussed is the role of **vertical shear of the mean wind-vector (i.e. turning of the wind vector with height)** on the organization of deep convection, in particular focusing on the production of **rotating updraughts** in a thunderstorm. Tornado-producing **super cell thunderstorms** arise only in a potentially unstable environment with large wind shear and, in the northern hemisphere, clockwise turning of the wind vector with increasing height.

Further reading

Book

Markowski, P.M., and Y.P. Richardson, 2010: **Mesoscale Meteorology in Midlatitudes**. John Wiley, 430 pp. (part 3).

Article

van Delden, A., 2001: The synoptic setting of thunderstorms in Western Europe. **Atmospheric Research**, **56**, 89-110.

List of problems (chapter 4)

This is the November 2014 edition of chapter 4 of the lecture notes on Atmospheric Dynamics., by Aarnout van Delden (IMAU, Utrecht University, Netherlands, a.j.vandelden@uu.nl).